Accepted Manuscript

Differential expression of novel metabolic and immunological biomarkers in oysters challenged with a virulent strain of OsHV-1

Tim Young, Aditya Kesarcodi-Watson, Andrea C. Alfaro, Fabrice Merien, Thao V. Nguyen, Hannah Mae, Dung V. Le, Silas Villas-Bôas

PII: S0145-305X(16)30481-5

DOI: 10.1016/j.dci.2017.03.025

Reference: DCI 2858

To appear in: *Developmental and Comparative Immunology*

Received Date: 10 December 2016

Revised Date: 30 March 2017

Accepted Date: 30 March 2017

Please cite this article as: Young, T., Kesarcodi-Watson, A., Alfaro, A.C., Merien, F., Nguyen, T.V., Mae, H., Le, D.V., Villas-Bôas, S., Differential expression of novel metabolic and immunological biomarkers in oysters challenged with a virulent strain of OsHV-1, *Developmental and Comparative Immunology* (2017), doi: 10.1016/j.dci.2017.03.025.

Graphical abstract

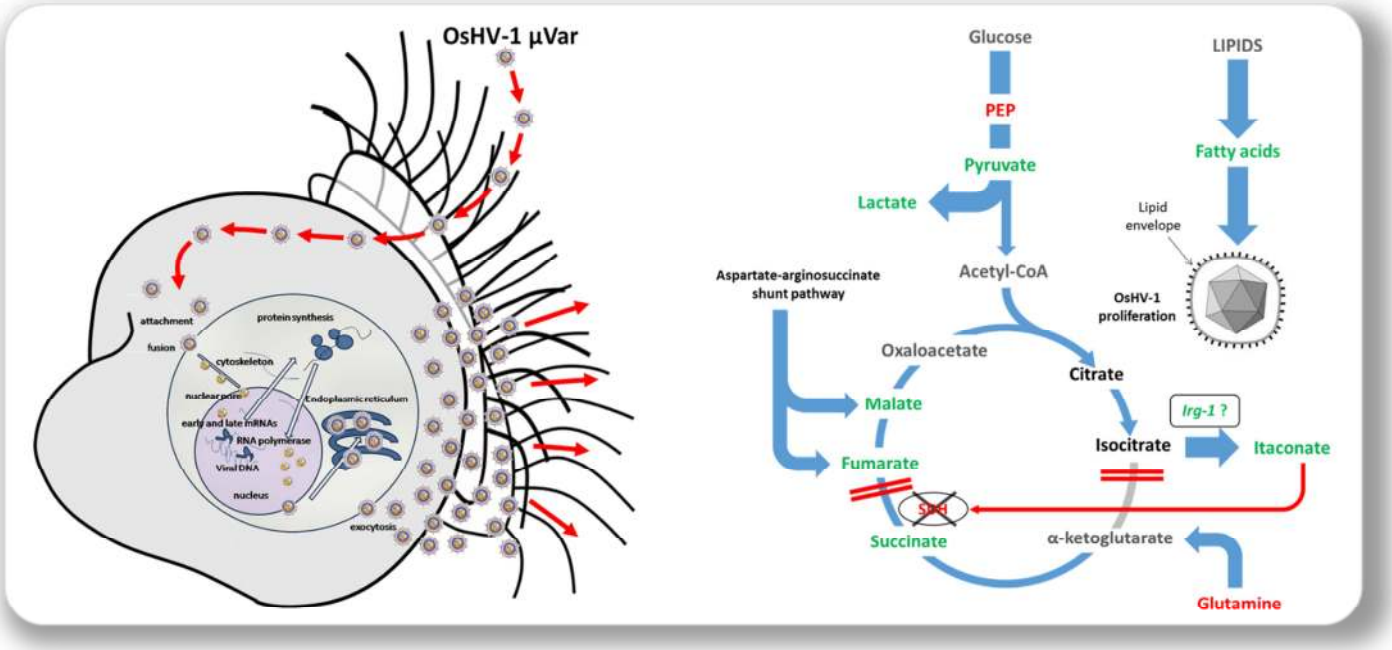

Differential expression of novel metabolic and immunological biomarkers in oysters challenged with a virulent strain of OsHV-1

Running Head: Oyster larval immunology

TIM YOUNG[a,b]
ADITYA KESARCODI-WATSON[c]
ANDREA C. ALFARO[a]
FABRICE MERIEN[d]
THAO V. NGUYEN[a]
HANNAH MAE[c]
DUNG V. LE[a]
SILAS VILLAS-BÔAS[b]

[a]Institute for Applied Ecology New Zealand, School of Science, Faculty of Health and Environmental Sciences, Auckland University of Technology, Private Bag 92006, Auckland 1142, New Zealand

[b]Metabolomics Laboratory, School of Biological Sciences, The University of Auckland, Private Bag 92019 Auckland Mail Centre, Auckland 1142, New Zealand

[c]Cawthron Institute, 98 Halifax Street East , Private Bag 2, Nelson 7042, New Zealand

[d]AUT-Roche Diagnostics Laboratory, School of Science, Faculty of Health and Environmental Sciences, Auckland University of Technology, Private Bag 92006, Auckland 1142, New Zealand

Corresponding author
Andrea C. Alfaro
Phone: +64-9-921-9999 ext. 8197
Fax: +64-9-921-9743
andrea.alfaro@aut.ac.nz

ABSTRACT

Early lifestages of the Pacific oyster (*Crassostrea gigas*) are highly susceptible to infection by OsHV-1 µVar, but little information exists regarding metabolic or pathophysiological responses of larval hosts. Using a metabolomics approach, we identified a range of metabolic and immunological responses in oyster larvae exposed to OsHV-1 µVar; some of which have not previously been reported in molluscs. Multivariate analyses of entire metabolite profiles were able to separate infected from non-infected larvae. Correlation analysis revealed the presence of major perturbations in the underlying biochemical networks and secondary pathway analysis of functionally-related metabolites identified a number of prospective pathways differentially regulated in virus-exposed larvae. These results provide new insights into the pathogenic mechanisms of OsHV-1 infection in oyster larvae, which may be applied to develop disease mitigation strategies and/or as new phenotypic information for selective breeding programmes aiming to enhance viral resistance.

Keywords: Aquaculture, *Crassostrea gigas*, Larvae, Metabolism, Metabolomics, Ostreid herpesvirus

1. INTRODUCTION

With an estimated value of $4.17 billion USD (FAO 2016), oysters are one of the most commercially important groups of aquatic organisms in the world. In 2014, global aquaculture harvests reached 5.2 million tonnes, representing one third of all cultivated marine molluscs. Although total production volume remains high, growth of the industry has been severely hampered in recent years by extreme disease outbreaks during warmer summer months. Ostreid Herpesvirus (OsHV-1) is a new and emerging viral disease of several molluscan taxa, including oysters (Batista et al. 2015; Sanmartín et al. 2016), scallops (Arzul et al. 2001; Ren et al. 2013), and clams (Xia et al. 2015a; Bai et al. 2016). OsHV-1 has also

been detected in mussels, but without signs of infectivity or adverse consequences (Burge et al. 2011; Domeneghetti et al. 2014), making them a potential reservoir for the virus. Over the past couple of decades, OsHV-1 has been widely associated with mass mortalities of farmed oysters around the globe. A growing number of epidemiology studies and experimental trials suggest that the virus is a causal factor in these events (Friedman et al. 2005; Burge et al. 2007; Segarra et al. 2010; Garcia et al. 2011; Schikorski et al. 2011a,b; Dégremont et al. 2015a,b). With stock losses of up to 100%, economic and social consequences due to the spread of the disease have been devastating in countries such as France, Ireland, USA, China, Australia and New Zealand where oyster aquaculture is a vital primary industry (Burge et al. 2006; Lewis et al. 2012; Castinel et al. 2015). From the perspectives of many scientists, farmers and stakeholders alike, OsHV-1 has been articulated to represent the biggest individual threat to oyster production that the sector has ever faced (Lewis et al. 2012; Castinel et al. 2015).

First evidences for the presence of herpesvirus genetic material in bivalves was obtained in 1976 from samples of *Ostrea edulis* in the UK (Davison et al. 2005). However, widespread detection of herpesviruses and associations with mass mortalities of shellfish were not apparent until the early 1990's (Renault et al. 1995). During the following decade, many occurrences of viral infections were documented around the world, and by 2005 molecular characterisations had led to the designation of the pathogen as the OsHV-1 reference genotype (GenBank accession no. AY509253.2) (Renault & Arzul 2001; Davison et al. 2005). More recently, there has been an emergence of numerous OsHV-1 variants affiliated with mortalities in different bivalve species displaying different epidemiological characteristics, and it appears that OsHV-1 is undergoing rapid evolution (Grijalva-Chon et al. 2013; Renault et al. 2014; Bai et al. 2015; Martenot et al. 2015). In 2008, the detection of a highly virulent new strain, OsHV-1 µVar (GenBank accession no. HQ842610.1), was

79 described in association with massive losses of oyster spat in France, Ireland and the UK
80 (Segarra et al. 2010). By 2010, this new variant had reached the coasts of Australia and New
81 Zealand, killing huge numbers of oyster stock within days and leading to sector collapses in
82 certain regions over the following few years (Jenkins 2013; Keeling et al. 2014). Between
83 2011 and 2013, genetic analysis of cultured oysters from China, Korea and Japan revealed
84 widespread herpesvirus infections from numerous genotypes across the East Asiatic region
85 (Shimahara et al. 2012; Hwang et al. 2013; Jee et al. 2013; Bai et al. 2015, 2016). High
86 mortalities associated with OsHV-1 µVar were observed in Swedish and Norwegian
87 hatcheries towards the end of 2014 (Mortensen et al. 2016). More recently, a new outbreak in
88 Tasmania in 2016 has crippled the Australian oyster aquaculture sector and its selective
89 breeding program (Davis 2016; Milne 2016; Whittington et al. 2016). Thus, it is clear that the
90 extent of this new variant's geographical reach is indeed a major global concern.
91 Due to the widespread prevalence and substantial socioeconomic consequences of
92 OsHV-1 µVar, it is vital that knowledge of the interactions between the virus and its hosts are
93 obtained to better understand pathogenesis of the disease, develop mitigation strategies, and
94 guide management decisions. To provide such knowledge, a series of focused research
95 themes relating to the spread of the virus and its mechanisms of infection have been
96 conducted in recent years including genotyping and phylogenetics (Renault et al. 2012;
97 Martenot et al. 2015; Mineur et al. 2015; Burioli et al. 2016), development of experimental
98 infection models (Paul-Pont et al. 2015), modes of transmission (Burge & Friedman 2012;
99 Lionel et al. 2013; Petton et al. 2013; Evans et al. 2016), viral replication and virulence
100 processes (Segarra et al. 2014a, 2016; Green et al. 2015; Martenot et al. 2016), antiviral
101 features of immunity and host responses at transcriptomic and proteomic levels (Renault et al.
102 2011; Corporeau et al. 2014; Green et al. 2014a,b; Normand et al. 2014; Segarra et al.
103 2014a,b; He et al. 2015) and identification of virus-resistant traits for selective breeding trials

104 (Dégremont 2013; Dégremont et al. 2015a,b). Most of these studies have focused on post-
105 metamorphic life stages. However, size and age are significant factors in viral susceptibility
106 and pre-metamorphic larval forms appear to be more vulnerable than their juvenile or adult
107 counterparts (Oden et al. 2011; Dégremont 2013; Paul-Pont et al. 2013; Azéma et al. 2016;
108 Dégremont et al. 2016).

109 Many oyster farms rely on large-scale hatchery production of larvae to supply spat for
110 growout, with increasing demand and stakeholder interests to enhance larval production
111 capacities (Barnard 2014). Thus, it is essential that we extend our knowledge to characterise
112 the pathophysiology of the disease during early ontogeny. Furthermore, the impacts of
113 OsHV-1 µVar on the health of wild populations and their connectivity through larval
114 mortalities, altered larval dispersal potentials, and reduced spat-falls are almost wholly
115 unknown, but are likely to be substantial (Dégremont et al. 2016). In order to assess the
116 ecological consequences of the disease and understand natural vectors and boundaries which
117 may influence its spread, it is important to focus research across all developmental stages. In
118 addition, the identification of specific genotypic and phenotypic traits in larvae which reflect
119 disease susceptibility/resistance would be highly beneficial for monitoring early outcomes of
120 selective breeding programs. Detailed physiological analysis of the host-virus interaction via
121 use of –omics technologies (e.g., transcriptomics, proteomics and metabolomics) may
122 provide fruitful for discovering such traits (Gómez-Chiarri et al. 2015). There are very few
123 studies which have focused on the highly susceptible pre-metamorphic life-stage and, to our
124 knowledge, none which have utilised metabolomic-based approaches to better understand the
125 physiological effect of OsHV-1 infection on homeostatic control mechanisms of metabolism
126 and immunity.

127 Metabolomics is a newly developing and rapidly advancing field under the –omics
128 banner which aims to provide global snapshots of alterations in the metabolite, or small

129 molecule (<1 KDa), cellular component (Holmes et al. 2008). Metabolites are the ultimate
130 end-products of gene expression and are strongly influenced by endogenous regulatory
131 mechanisms, as well as by external elements (Fiehn 2002). As intermediates of metabolism,
132 metabolites comprise the available biochemical depot of macromolecular precursors and
133 energy transfer molecules required for optimal organismal growth and functioning. Thus, the
134 composition of the metabolite pool and their flux dynamics provide a closer representation of
135 an organism's phenotype than molecular features at other levels of biological organisation,
136 such as gene transcripts, which may display considerable temporal variations in expression
137 compared to the final phenotypic response, or be entirely decoupled from downstream
138 metabolic processes (Cascante & Marin 2008; Winter & Krömer 2013; Feussner & Polle
139 2015). With many recent applications across the life sciences (e.g., functional genomics
140 [Sévin et al. 2015], selective breeding [Hill et al. 2015; Hong et al. 2016], aquaculture-related
141 research [Young et al. 2015, 2016; Alfaro & Young 2016], toxicology [Bouhifd et al. 2013;
142 Størseth & Hammer 2014; Chen et al. 2016a] and disease diagnostics, monitoring and
143 prevention [Pallares-Méndez et al. 2016; Wishart 2016]), metabolomics is proving extremely
144 valuable as a highly efficient approach for generating new hypotheses and deciphering
145 complex metabolic and gene regulatory networks of vertebrate and invertebrate models.
146 By scanning broad sets of metabolic features in whole organisms, tissues or biological
147 fluids in response to environmental influences, such as bacterial or viral infections,
148 metabolomics-based approaches can provide novel information to gain insights into the
149 mechanisms of disease progression, resistance and remediation in aquatic organisms
150 (reviewed by Alfaro & Young 2016; Young & Alfaro 2016). For example, metabolomics has
151 recently been successfully applied to identify biomarkers for *Vibrio* spp. infections in mussels
152 and crabs (Wu et al. 2013; Ellis et al. 2014; Su et al. 2014; Ye et al. 2016), to gain detailed
153 metabolic information on tissue-specific host responses of shrimp and crayfish to white spot

154 syndrome virus (Liu et al. 2015; Chen et al. 2016b; Fan et al. 2016), and to develop practical
155 treatment methods for streptococcal disease in fish (Ma et al. 2015; Zhao et al. 2015).
156 Although limitedly applied to the investigation of marine invertebrate early life stages thus
157 far, metabolomics has great potential to provide new insights into the interactions between
158 OsHV-1 µVar and its oyster larval hosts. Thus, we have conducted the first metabolomics
159 study to assess gross compositional alterations within the oyster larval metabolome in
160 response to OsHV-1 infection.

161 **2. METHODS**

162 Refer to the Supplementary Methods file for detailed method descriptors.

163 **2.1 Larval challenge**

164 OsHV-1 µVar inoculum was prepared from oysters that had been stored at −80°C and
165 previously tested positive by qPCR (primers: GTCGCATCTTTGGATTTAACAA [BF] and
166 ACTGGGATCCGACTGACAAC [B4], after Martenot et al. [2010]). A whole tissue
167 homogenate was filtered and the virus concentration was determined via qPCR using BF and
168 B4 primers in a SYBR Green assay. Oyster larvae were produced from selectively bred
169 broodstock maintained by the Cawthron Institute (Nelson, New Zealand) and reared in a 170
170 L conical flowthrough tank to 16 days post-fertilisation, using standard industry protocols. A
171 cohort of healthy larvae was distributed among 12 × 2L beakers containing sterile synthetic
172 seawater, at a density of 7 larvae mL^{-1}. OshV-1 inoculum was added to six beakers at a
173 concentration previously determined to cause mortality, with the remaining beakers serving
174 as negative controls (i.e., six replicates per treatment). After 48 hrs, behavioural observations
175 were made and all larvae were snap frozen and stored at –80°C until metabolite analysis.

176 **2.2 Metabolite extraction, analysis and identification**

177 Metabolites were co-extracted with an internal standard using a cold methanol-water method
178 and derivatised via methyl chloroformate (MCF) alkylation according to Villas-Bôas et al.
179 (2011), then analysed via gas chromatography mass spectrometry (Thermo Trace GC Ultra
180 system) according to Smart et al. (2010). Deconvolution of chromatographic data was
181 performed using the Automated Mass Spectral Deconvolution and Identification System
182 (AMDIS v2.66) software. Metabolites were identified using Chemstation software (Agilent
183 Technologies) and customised R xcms-based scripts (Aggio et al. 2011) to interrogate an in-
184 house library of MCF derivatised compounds.

185 **2.3 Statistics**

186 Peak intensity data were normalised against the internal standard and by sample-specific
187 biomass, prior to being autoscaled. All statistical analyses were conducted using
188 Metaboanalyst 3.0 (Xia et al. 2015b). Univariate analyses were performed to screen
189 metabolite profile differences between controls and treatments, including foldchange
190 analysis, students *t*-test , Significant Analysis of Metabolites/Microarrays (SAM) and
191 Empirical Bayes Analysis of Metabolites/Microarrays (EBAM). Agglomerative Hierarchical
192 Cluster Analysis (HCA), *k*-means clustering (*k*MC) and Principal Components Analysis
193 (PCA) were used as unsupervised multivariate cluster analyses to identify natural groupings
194 of samples based on the underlying structure of the data. Projection to Latent Structures
195 Discriminant Analysis (PLS-DA) and Random Forrest (RF) analysis were used as supervised
196 multivariate classification analysis methods. The PLS-DA model was validated using Leave
197 One Out Cross Validation (LOOCV), the model performance was assessed via R^2 and Q^2
198 values, and important classifiers were identified via their Variable Importance in Projection
199 (VIP) scores. RF Receiver Operator Characteristic (ROS) curves were generated by Monte-

Carlo Cross Validation (MCCV) using balanced subsampling. Quantitative Enrichment Analysis (QEA [Xia & Wishart 2010]) and Network Topology Analysis (NTA [Nikiforova & Willmitzer 2007]) were used as pathway analysis methods to investigate functional relationships among the annotated metabolites. Biochemical pathways in the Kyoto Encyclopedia of Genes and Genomes database (Kanehisa & Goto 2000) involving two or more annotated metabolites with simultaneous QEA *p*-values < 0.05, QEA false discovery rates [FDRs] < 0.1, and with NTA Pathway Impact (PI) scores > 0.1 were considered as potential primary target pathways of interest. Correlation analysis was used to identify major differences in pairwise metabolite correlations (Pearson). Correlation Network Analysis (CNA) was performed to provide enhanced visualisation of metabolite relationships using Cytoscape 3.0 software (Shannon et al. 2003) and the ExpressionCorrelation plugin (Karnovsky et al. 2012).

3. RESULTS

The metabolite profiles of oyster larvae exposed to OsHV-1 µVar were compared to those from non-exposed control larvae in order to gain insights into the pathogenic mechanisms of infection. Observations of larval behaviour were made every 12 hrs during the trial until first signs of differences between virus-exposed larvae and controls were discerned, i.e., changes in swimming speeds, trajectories and distributions within the water column. After 48 hrs, organisms that had been challenged with OsHV-1 µVar tended to be aggregated in the lower 30–50% of the water columns compared to control larvae which were more evenly distributed. When examined under the microscope, virus-exposed larvae also displayed slower motility and abnormal swimming patterns (i.e., horizontal planar circular motions rather than random) characteristic of OsHV-1 infections reported previously (Burge & Friedman 2012; DoA 2015; OIE 2016). However, larval coloration (a commonly used crude

assessment which can indicate severe poor health status) generally appeared to be visually similar between treatments. Mortality assessments revealed that 100% of oyster larvae in all beakers were alive at the time of sampling for metabolomics.

3.1 Univariate analysis

GC-MS analysis of larval extracts detected a total of 105 unique metabolites after QC filtering of the data. Of these, 75 were attributed specific chemical identities by matching chromatographic and mass spectral information against our in-house metabolite library (Supplementary Table 1). The remaining 30 features are currently listed as 'unknowns' since no matches were found (Supplementary Table 2). Univariate statistical analyses showed a number of differences in the metabolite profiles between control and virus-infected larvae (Figure 1). SAM identified 30 metabolites as being differentially ($p < 0.05$) expressed between larvae exposed to OsHV-1 µVar and control larvae with an FDR of 3.1% (Figure 1A), whereas EBAM identified 28 metabolites as being differentially expressed with an FDR of 4.7% (Figure 1B). The summarised results of student's *t*-test, SAM and EBAM are displayed in Figure 1C, along with their relative fold changes. Taking the results of these analyses together, the abundances of nine metabolites were likely under expressed in virus-infected larvae compared to the metabolic baseline of control organisms, and 20 metabolites were likely over expressed. Full details of the univariate statistical analyses are provided in Supplementary Tables 1 and 2.

3.2 Unsupervised multivariate cluster analysis

Unsupervised multivariate analyses of entire metabolite profiles revealed that good separation between control and virus-infected larvae could be obtained based on the underlying structure of the data (Figure 2). HCA correctly positioned samples into two main groups (group 1, controls $n = 6$; group 2, treatment $n = 6$) (Figure 2A), indicating that the

248 within-class variation was considerably lower than the between-class variation. *k*MC
249 corroborated this by also correctly assigning larval samples into groups based on the
250 treatment that they received (Figure 2B; inserted table). PCA produced a 2-D score plot
251 containing two distinct clusters of samples which appropriately reflected their class labels and
252 with no indication of sample outliers (Figure 2C). The two clusters are separated along PC1
253 with the relative abundances of around 40 metabolites explaining much of the divide (see
254 Supplementary Tables 1 and 2 for the PCA loadings). Although the calculated 95%
255 confidence interval ellipses overlapped, the accumulative variation among all samples
256 explained by PC1 and PC2 was only 46.0%. It is therefore possible that the OsHV-1 µVar-
257 infected larval samples may be separated from control samples along other PC vectors not
258 discernible in the 2-D score plot which might be revealed via supervised multivariate
259 techniques.

260 **3.3 Supervised multivariate classification analysis**

261 Supervised multivariate classification analysis was clearly able to discriminate larval
262 samples based on the treatment they received (Figure 3). Compared to PCA, the 2-D PLS-DA
263 score plot better separated virus-infected from control larval samples along the x-axis (Figure
264 3A), with good cross-validated model performance using the first two latent variables
265 (Accuracy = 100%; R^2 = 96.9%; Q^2 = 79.6%) (Figure 3B). PLS-DA additionally informed
266 upon which metabolites were most important for the classification model via their VIP scores
267 (Figure 3C). Significant classifiers for the separation between virus-infected and control
268 groups were ranked, yielding 43 metabolites (35 annotated and 8 unannotated) with VIP
269 scores > 1.0 (Figure 3C and Supplementary Tables 1 and 2). In addition to the 30 differing
270 metabolite abundances identified via SAM and/or EBAM (Figure 1C), PLS-DA also

recognised 2-aminobutyric acid, glycine, hexanoic acid, homocysteine, putrescine, valine, and four additional unannotated metabolites as being important classifiers.

The RF machine learning algorithm was further employed as a complimentary feature selection method to similarly rank the most salient metabolite features responsible for class separation via a different statistical approach more resistant to over fitting than PLS-DA (Figure 4). A default RF classification model was first constructed using ten features (i.e., ~ $\sqrt{n}$) and 500 permutations, which correctly classified all samples. A series of ROC curve analyses were then performed to generate various *n*-feature classification models which were validated using MCCV sub-sampling to assess predictive accuracies (Figure 4A). The predictive accuracies of the 5-, 10-, and 15-feature RF models were 94.5, 98.0, and 100%, respectively, with AUC's of 0.985, 1.0, and 1.0, respectively (Figure 4B). ROC curve analysis of the 5-feature model with corresponding confidence intervals is shown in Figure 4C, and the predicted class probabilities of the model is shown in Figure 4D. The average importance and selected frequencies of metabolites in the 5-feature RF model are shown in Figure 4E and Figure 4F, respectively. Most metabolites identified as potential biomarker candidates via SAM, EBAM and PLS-DA were also selected to some degree by RF which further corroborates their significance as key classifiers of larval health condition. The most frequently selected compounds (> 20%) with high measures of average importance (> 1.0) were fumaric acid, 4-hydroxyphenylacetic acid, glutamine, glutaric acid, myristic acid, 2-aminoadipic acid, and two unannotated metabolites. As indicated by RF, a low error of classification could be obtained with few compounds.

3.4 Functional biochemical pathway analysis

Based on the profiles of annotated metabolites, metabolic pathway analyses were performed to reveal the most relevant pathways related to the pathophysiology of oyster larvae exposed

to OsHV-1 µVar (Figure 5) (see Supplementary Table 3 for full analysis details). A total of 43 biochemical pathways were recognised from within the KEGG database which contained one or more of the annotated metabolites detected. Pathways involving two or more detected metabolites and with simultaneous QEA *p*-values < 0.05, QEA FDR values < 0.1, and NTA Pathway Impact (PI) values > 0.1 were screened as potential primary target pathways of interest relating to the treatment effect. According to these selection criteria, 12 biochemical pathways were identified with evidence of metabolic disturbances in virus-exposed larvae (Figure 5A), comprising of: glycolysis/gluconeogenesis; pyruvate metabolism; tricarboxylic acid cycle; glyoxylate and dicarboxylate metabolism; aminoacyl-tRNA biosynthesis; tyrosine metabolism; alanine, aspartate and glutamate metabolism; arginine and proline metabolism; glycine, serine and threonine metabolism; cysteine and methionine metabolism; D-glutamine and D-glutamate metabolism; and nicotinate and nicotinamide metabolism. Nine further pathways that were identified statistically via QEA ($p < 0.05$) but did not meet one or more of our other ideal impact assessment criteria were screened as potential secondary target pathways of interest, comprising of: purine metabolism; pyrimidine metabolism; tryptophan metabolism, lysine degradation; nitrogen metabolism; fatty acid biosynthesis; fatty acid elongation in mitochondria; biosynthesis of unsaturated fatty acids, and fatty acid metabolism.

3.5 Correlation analysis

Pairwise metabolite–metabolite correlation matrices of Pearson coefficients for each treatment group were separately constructed and displayed at heatmaps (Figure 6). In general, substantial treatment-induced differences in the relationships between metabolites were exposed, as demonstrated by the many contrasting colours of same cells between the two heatmaps. From these totals of 5565 pairwise comparisons within each dataset, 167 strong

linear correlations (R^2 values > 0.7 or < –0.7) were found to be highly differentially expressed (i.e., positive vs negative relationships) between larvae infected with OshV-1 µVar and baseline controls. Correlation network analyses (CNA) with selection criteria of R^2 > 0.9 or < –0.9 were then separately performed on control and virus-exposed larval datasets to summarise and reveal the major correlation differences in the metabolic networks (Figure 7).

4. DISCUSSION

The aim of this study was to evaluate changes in the *C. gigas* oyster larval metabolome induced by ostreid herpesvirus and determine whether metabolomics-based approaches can deliver novel mechanistic insights into immunological defence systems of early life-stage marine invertebrates. Thus, we performed a comprehensive determination of metabolic alterations in oyster larvae exposed to the newly emerging and highly virulent OsHV-1 µVar genotype via GC/MS-based metabolomics. Our findings revealed that viral exposure had an effect on many metabolites involved in central carbon metabolism, across broad chemical classes with various functional roles. These virus-induced changes in the metabolite profiles enabled us to discriminate healthy from unhealthy larvae via multivariate clustering and classification techniques, discern relationships among metabolites, identify entire biochemical pathways evidenced of being altered, and further focused our attention towards specific mechanisms of immunity characteristic of the pathophysiological condition. We identified coordinated changes in tricarboxylic acid (TCA) cycle-related metabolites in virus-exposed larvae indicative of abnormal energy metabolism and biosynthesis of an antimicrobial product, and also detected subtle signs of potential oxidative stress, transformation or degradation of extracellular matrix scaffolding, and disruption of normal lipid metabolism suggestive of requirements for viral appropriation of host-cell biomaterial, among other processes. Confirmation of these hypotheses based on the metabolomics data

will require further investigation using functional assays at other levels of biological organisation.

4.1 Lipid metabolism

Enveloped viruses, such as those from the herpesviridae family, are known to physically and metabolically remodel host cells during infection to create optimal environments for their replication by manipulating lipid signalling and metabolism (Chukkapalli et al. 2012; Rosenwasser et al. 2016). Such viruses instructively alter host metabolism in order to supply the high quantities of fatty acids which are required as vital lipid envelope components during virion assembly (Koyuncu et al. 2013). Although the precise induction mechanisms have not yet been elucidated, enrichment of host fatty acid (FA) production is a common response of different organisms to infection by various enveloped viruses (Mazzon & Mercer 2014; Hsieh et al. 2015; Sanchez & Lagunoff 2015), including herpes-type viruses such as human cytomegalovirus (HMCV) (Spencer et al. 2011; Seo et al. 2013; Purdy et al. 2015) and Kaposi's sarcoma-associated herpesvirus (Bhatt et al. 2012). An emerging theme is that these lipid-modifying pathways are linked to innate antiviral responses which can be modulated to inhibit viral replication (Chukkapalli et al. 2012). For example, HCMV stimulates free fatty acid (FFA) production to enable and enhance assembly of infectious virions by activating expression of *ACC1* host mRNA, the gene encoding for the rate-limiting enzyme acetyl-CoA carboxylase (ACC) involved in the initial commitment stage of *de novo* FA synthesis (Spencer et al. 2011); whereas pharmacological inhibition of host ACC substantially limits the ability of HCMV to replicate (Munger et al. 2008). More recently, Koyuncu et al. (2013) reported that siRNA-induced knockdown of a suite of other enzymes involved in FA synthesis (fatty acyl-CoA synthetases and elongases) inhibited herpesvirus replications, whereas knockdown of proteins responsible for FA catabolism (the peroxisomal β-oxidation

367 enzyme acetyl-CoA acyl-transferase 1) and the first step of triglyceride synthesis (1-
368 acylglycerol-3-phosphate O-acyltransferase 9) enhanced viral replication by elevating the
369 available FFA pool. Thus, the FA synthesis pathway is currently gaining considerable
370 attention as a prime target for the development of innovative therapeutics that are not
371 dependent on mechanisms of adaptive immunity, and therefore resilient to emerging virus
372 variants which have become resistant to anti-viral therapies (Goodwin et al. 2015).
373 Looking at the global metabolic changes in larvae induced by OsHV-1 µVar
374 exposure, there was a signature consisting of FFAs, presumably involving either a change in
375 the relative rates of production and/or breakdown. These variation patterns contributed
376 towards earmarking FA pathways (FA metabolism, FA β-oxidation and FA elongation in
377 mitochondria) as being candidate targets of interest in our study via secondary bioinformatics
378 techniques, and also were key metabolites causative to the perturbations observed within the
379 differential metabolic correlation networks. Under the starvation conditions we employed
380 during the viral challenge, an effect on basal lipolysis would be the most obvious potential
381 mechanism for the FFA changes observed here. Compared to non-infected control larvae, the
382 general increase in medium and long chain FFAs (C16:0, C18:3n-6, C20:4n-6, C20:5n-3,
383 C22:2n6, C22:6n-3) and microalgal-derived dietary FFAs (C14:0, C16:1n-7) in virus-infected
384 larvae are indicative of enhanced catabolism of endogenous triacylglycerol lipid supplies.
385 This pre-metamorphic host-response appears to be somewhat similar to that of post-
386 metamorphic life stages. Proteomic-based analyses of adult Pacific oysters experimentally
387 infected with OsHV-1 µVar recently identified that a key enzyme involved in the first step of
388 lipid hydrolysis, triacylglycerol lipase (TGL), was over-accumulated in virus-exposed
389 animals which likely reflects enhanced lipolysis during initial stages of infection (Corporeau
390 et al. 2014). Furthermore, transcriptomic-based analyses revealed over-expression of genes
391 encoding for TGL and phospholipase A2 (an enzyme that releases FAs from the second

carbon group of glycerol in phospholipids) in OsHV-1 µVar-infected oysters (He et al. 2015), and several other studies also report triglyceride levels being substantially decreased in juvenile and adult oyster hosts exposed to the virus (Pernet et al. 2010, 2014; Tamayo et al. 2014). In adult oysters, FFA accumulations do not appear to coincide with the reduced lipid contents following OsHV-1 µVar infection likely due to them being transitory intermediates (Tamayo et al. 2014), for which simultaneously enhanced rates of β-oxidation could explain. However, infected adult oysters display a down-accumulation in fatty acid-binding protein (FABP) (Corporeau et al. 2014), a chaperone involved in trafficking FFAs across the mitochondrial membrane, and, at the height of the viral load, decreased *Fabp* transcription and expression of a gene encoding the alpha subunit of FA oxidation complex (He et al. 2015), all of which would limit β-oxidation rather than promote it. Thus, aside from being used for host energy metabolism, the FFAs produced during virus-induced lipolysis in oysters may be used as precursor synthesis molecules for constructing the lipid envelope during virus assembly and proliferation; as previously reported for HCMV infections.

Although FFA levels at a particular time reflect the complex metabolic balance between lipolysis, β-oxidation, and any other FA production (e.g., *de novo* synthesis) or consuming processes (e.g., triglyceride synthesis and utilisation for virion assembly), the FFA accumulations we observed are consistent with the general findings of other studies which have investigated various models of herpes-type infections. Perhaps a key point of difference in host-virus interactions between OsHV-1 and vertebrate-infecting herpesviruses could be the primary source from which the FAs are derived from (i.e., lipolysis vs *de novo* synthesis). We recommend that targeted analyses of these pathways are additionally conducted at transcriptional and translational levels, in combination with metabolite profiling, in order to tease out the mechanistic intricacies of OsHV-1 µVar-induced modulation of host lipid metabolism in oyster larvae. With FAs being necessary components required for OsHV-

1 replication and proliferation, establishing the precise viral targets of host lipid metabolism could assist in the development of antiviral therapeutics, and/or identification of unique disease resistant genomic or metabolic traits for selective breeding purposes.

4.2 TCA cycle and immunoresponsive gene 1

Host metabolism changes are suggestive of immunoresponsive gene 1 (*Irg1*) like activation, which directly affects carbon flux through the TCA cycle and modifies energy metabolism. *Irg1* is commonly and highly expressed in vertebrate macrophages during inflammation and infection by a variety of pathogens (Preusse et al. 2013). *Irg1* encodes immune-responsive gene 1 protein/ *cis*-aconitic acid decarboxylase (IRG1/CAD) which links cellular metabolism with immune defence by catalysing the decarboxylation of *cis*-aconitic acid (the citrate → isocitrate isomerisation intermediate in the TCA cycle) to itaconic acid (ITA) (Michelucci et al. 2013; Vuoristo et al. 2015). ITA is a metabolite with potent antimicrobial properties (Naujoks et al. 2016), and was identified in our study as being over-accumulated in virus-exposed oyster larvae. ITA being discovered as the gene product of *Irg1* is arguably one of the most important biological insights made in recent times (Sévin et al. 2015), and was only revealed through taking a non-hypothesis driven metabolomics profiling approach as we have in the current study. ITA has newly been recognised as a crucial regulatory metabolite involved in posttranscriptional mechanisms of reprogramming mitochondrial metabolism through modulation of substrate level phosphorylation, TCA cycle flux and succinic acid signalling (Mills & O'Neill 2016; Cordes et al. 2016; Németh et al. 2016), production of inflammatory cytokines (Lampropoulou et al. 2016) and its ability to alter cellular redox balance (Tretter et al. 2016).

Upregulation of *Irg1* transcription leads to a characteristic metabolic signature of a "broken TCA cycle" in stimulated macrophages (O'Neill 2015; O'Neill & Pearce 2016;

O'Neill et al. 2016). ITA accumulation represents the first of two distinctive break-points in the pathway due to decreased transcription of isocitrate dehydrogenase (IDH; catalyses isocitrate → α-ketoglutarate), and the redirection of *cis*-aconitic acid metabolism via enriched *Irg1*-encoded IRG1/CAD expression (Jha et al. 2015; Yanamoto et al. 2015). The increased production of ITA decreases citric acid oxidation through the cycle. To compensate for the reduced flux under such conditions, Maisser et al. (2016) showed that glutamine uptake is co-enhanced with *Irg1* expression, serving to replenish the pathway with α-ketoglutaric acid through glutaminolysis. In agreement, the reduction in free glutamine content that we observed in OsHV-1 µVar-exposed larvae is consistent with such an anaplerotic mechanism. Herpes-infected human cells can switch substrate utilisation from glucose to glutamine to accommodate the biosynthetic and energetic needs of the viral infection, and allow glucose to alternatively be used biosynthetically (Chambers et al. 2010). Virus-induced reprogramming of glutamine metabolism and anaplerosis of the TCA cycle at this particular point appears to be critical for successful replication of herpes-type viruses, as well as maintenance of cellular viability during latent infections (Sanchez et al. 2015; Thai et al. 2015).

The second characteristic break-point in the TCA cycle occurs at succinate dehydrogenase/ respiratory Complex II (SDH/CII), the enzyme which catalyses the oxidation of succinate → fumarate, and also crucially regulates respiration in the electron transport chain (Mills & O'Neill 2016). ITA is a competitive inhibitor of SDH/CII (Cordes et al. 2016), and thus, when ITA levels increase, enzyme activity is attenuated leading to an accumulation of succinic acid and a concomitant decrease in oxidative phosphorylation (OxPhos) (Lampropoulou et al. 2016). Directly in line with this second TCA cycle break-point feature, oyster larvae exposed to OsHV-1 µVar exhibited elevated levels of succinic acid. The functional purpose of reprogramming host cell metabolism to accumulate succinic acid in response to pathogen infections appears to stem in part from its ability to mediate

466 inflammatory responses. Aside from having a fundamental role in the TCA cycle, succinic
467 acid can act as a regulatory signal, via succinate receptor 1 (GPR91/SUCNR1), to induce
468 production of pro-inflammatory cytokines (TNF-α, IL-1β) which can enhance immune-
469 stimulatory capacity, but also can exasperate disease when produced in excess (Rubic et al.
470 2008; Tannahill et al. 2013; Mills & O'Neill 2014; Littlewood-Evans et al. 2016).
471 GPR91/SUCNR1 is therefore involved in sensing the immunological danger exposed by
472 *Irg1*/ITA-induced succinic acid accumulations, thus further establishing direct links between
473 immunity and cellular respiration.

474 Rather than downstream TCA cycle intermediates being depleted as a consequence of
475 this second break at SDH/CII, the metabolic response involves enrichment of the aspartate-
476 arginosuccinate shunt pathway which provides a compensatory mechanism to replenish the
477 system (Jha et al. 2015), thus leading to significant increases in levels of fumaric and malic
478 acids regardless of SDH/CII inhibition (Lampropoulou et al. 2016). In agreement, both of
479 these TCA metabolites were over-accumulated in virus-exposed larvae. Thus, our metabolite
480 data suggest that larval oyster cells have a comparable host response to OsHV-1 µVar as
481 mammalian macrophages when stimulated or infected with other viruses. To the best of our
482 knowledge, this is the first report of such metabolic reprogramming of the TCA cycle in an
483 invertebrate with the specific metabolite signature of pathogen-induced *Irg1* transcription
484 directly in accordance with vertebrate cell models. How OsHV-1 might stimulate genomic
485 components leading to activation of *Irg1* transcription in oysters is not known, but would
486 likely share some parallels with mechanisms of higher taxa (see Owens & Malham 2015;
487 Naujoks et al. 2016; Tallam et al. 2016).

488 Only two cases of *Irg1* involvement in marine mollusc immune responses
489 have thus far been reported. Martín-Gómez et al. (2012) detected an up-regulation of *Irg1*
490 transcription in the flat oyster, *Ostrea edulis*, exposed to Bonamiosis disease under light and

heavy infection scenarios, which suggest that *Irg1* could play a role at early infection stages with prolonged expression at later stages. Furthermore, although not stated nor discussed in their manuscript, He et al. (2015 [supplementary material]) identified via untargeted gene expression profiling that the *C. gigas Irg1* transcript was over-expressed 9-fold in adult oysters exposed to OsHV-1 at the height of the viral replication process. In combination with our findings of a classic metabolic signature for *Irg1* over-expression and enhanced aconitase activity in virus-exposed larvae, these data are supportive of an active role of *Irg1* and its metabolic product, ITA, in the innate immunity of oysters, and further provide the first reports of such associated pathophysiological mechanisms of disease in marine invertebrates. Moreover, these data also suggest that this particular metabolic reprogramming mechanism develops very early in the oyster lifecycle, and is a conserved feature of immunity across the metamorphic boundary. These findings provide fresh insights into the early evolution of innate immunity. We suggest that a detailed characterisation of this system, including endogenous regulatory networks and exogenous effectors, be conducted through ontogeny which may provide useful information for identifying disease resistant traits. Investigation of other mechanisms associated with altered host energy metabolism, such as the Warburg effect, may also deliver important insights into the pathophysiology of the disease.

4.3 Warburg effect

The Warburg effect is an abnormal metabolic shift that was first discovered in proliferating cancer cells (Ferreira 2010). It has since been detected in vertebrate cells infected by viruses (Delgado et al. 2010, 2012; Darekar et al. 2012; Thai et al. 2014), and was recently implicated as an actuated pathway during viral infections in shrimp and oysters (Corporeau et al. 2014; Su et al. 2014; Hsieh et al. 2015; Fan et al. 2016; Li et al. 2016). Herpes-type viruses are known to activate oncogenes, thus providing a mechanistic link with cancerous

cell phenotypes (Mesri et al. 2014). The Warburg effect is distinguished by a high rate of glycolytic flux and unusual aerobic fermentation of glucose to lactic acid even though there is enough oxygen available for OxPhos to proceed (Kelly & O'Neill 2015). It is often accompanied by the activation or enrichment of other metabolic pathways that provide energy and direct the flow of carbon and nitrogen, such as the pentose phosphate pathway, nucleotide biosynthesis, lipolysis, and glutaminolysis (Zaidi et al. 2013; Tannahill et al. 2013; Su et al. 2014; Sanchez & Lagunoff 2015; Li et al. 2016), and also with mechanisms of innate immunity such as *Irg1* activation/ ITA over-accumulation (Kelly & O'Neill 2015).

Metabolic alterations characteristic of the Warburg effect involves increased glycolysis, elevated levels of lactic acid, and changes in rates of nicotinamide adenine dinucleotide phosphate (NADPH) production/utilisation. These effects result from the diversion of glucose metabolism, glutamine oxidation, and requirements of reducing equivalents for FA biosynthesis and for mounting anti-oxidant responses to Reactive Oxygen Species (ROS) via re-oxidisation of glutathione (vander Heiden et al. 2009; Weljie & Jirik 2011; Senyilmaz & Teleman 2015). Although the precise initiating mechanism/s responsible for reprogramming the glycolytic and gluconeogenic pathways that result in these metabolite changes are not yet completely understood (Vijayakumar et al. 2015), succinic acid accumulations act as an innate immunity regulatory signal to trigger a switch in core metabolism from OxPhos to glycolysis. Succinic acid stabilises the alpha subunit of hypoxia inducible factor 1 (HIF-1α) thereby activating transcription of genes which downregulates OxPhos (e.g., via indirect inhibition of pyruvate kinase to reduce TCA cycle flux), enhances glycolysis (e.g., via increased production of hexokinase and glucose transporters), and promotes lactic acid production (e.g., via regulation of lactate dehydrogenase and monocarboxylate transporter 4) (Ben-Shlomo et al. 1997; Selak et al. 2005; Semenza 2010; Palsson-McDemott & O'Neill 2013; Tannahill et al. 2013; Mills & O'Neill 2014). Thus, with

ITA-induced inhibition of SDH/CII, succinic acid may be an important metabolite linking *Irg1* activation with the Warburg effect in virus infected cells.

Compared to baseline control larvae, lactic acid was over-accumulated in OsHV-1 µVar-exposed larvae, whereas NADPH levels were lower. Secondary bioinformatics analysis of the metabolomics data also recognised glycolysis/gluconeogenesis and nucleotide metabolism as being differentially modulated as a larval host response to the virus, which could reflect an active Warburg-like effect. Our findings align with those of Corporeau et al. (2014) who utilised a proteomic-based approach to assess global protein changes in adult oysters infected with OsHV-1 µVar. Altered host protein expressions included changes in mitochondrial membrane permeability (accumulation of voltage-dependant anion channels [VDAC]), and enhanced glycolysis via an increase in the glycolytic enzyme Triose phosphate isomerase and decreases in the gluconeogenic enzymes Fructose 1,6-biphosphatase and Malate dehydrogenase (MDH); signatures which resemble induction of the Warburg effect (Chen et al. 2011; Maldonado & Lemasters 2012; Corporeau et al. 2014). Supporting the findings of Corporeau et al. (2014), increased and decreased expressions of genes encoding VDAC and MDH, respectively, were detected in adult oysters exposed to the virus (Renault et al. 2011; He et al. 2015). Taken together, these characteristic evidences at various levels of organisation (i.e., gene, protein and metabolite) suggest an involvement of the Warburg effect as a pathophysiological feature of OsHV-1 µVar infection.

It is thought that the Warburg effect in cancer cells is adapted to facilitate the uptake and incorporation of nutrients into the biomass needed to produce new cells during proliferation at the expense of efficient, albeit slow, ATP production via OxPhos (vander Heiden et al. 2009; Zhang et al. 2012). The functional purpose for selection of energy inefficient lactic acid fermentation over OxPhos in virus-exposed oysters is less clear. However, it is possible that the Warburg effect is ‘strategically’ induced by OsHV-1 as a

metabolic reprogramming mechanism beneficial to the pathogen. With the catabolism of glucose exceeding the bioenergetics needs of cells during Warburg activation (Thomas 2014), the high yields of intermediates created through enriched glycolysis and a truncated TCA cycle could be used for production of purine and pyrimidine nucleotides and other components required for viral DNA synthesis and envelope assembly. Aerobic fermentation would also provide energy for these processes more swiftly than through OxPhos and with less risk of constraining glycolytic flux via ATP-induced negative feedback inhibition (Zhang et al. 2012; Sanchez & Lagunoff 2015), thus facilitating rapid and persistent viral replication.

4.4 Oxidative stress

We hypothesised that significant changes in the abundances of metabolites reflective of oxidative stress would be represented in OsHV-1 Var-exposed oyster larvae. Exposure to invading pathogens initially triggers robust innate immune responses, and a rapid release of reactive oxygen species (ROS) called an oxidative burst is usually registered soon afterwards (Torres et al. 2006). ROS are beneficial since they can facilitate degradation of invading pathogen biomaterial, and also act as signalling molecules to potentiate other immune responses, such as activation of interferons and their regulatory factors (Chiang et al. 2006). However, when produced in excess, they can cause irreparable damage to crucial host cells through degradation of macromolecular cellular components, including lipids, proteins, and DNA (Pisoschi & Pop 2015). During viral infections, this can actually promote virus proliferation by enhancing dispersion from lysed or apoptotic cells (Stehbens 2004). Thus, oxidative bursts should ideally be reduced before attaining critical levels, and can be achieved through an intricate balance of co-regulated antioxidant processes. These include production of the antioxidant metabolite glutathione (GSH) and a number of enzymes which regulate GSH turnover, directly recycles ROS, or are involved in repairing ROS-induced damage

589 (Knight 2000; Apel & Hirt 2004). Adult and juvenile oysters exposed to OsHV-1, or showing
590 variable susceptibilities to disease associated with the virus, display differential expression of
591 these enzymes, and/or the genes which encode them (Fleury et al. 2010; Fleury & Huvet
592 2012; Schmitt et al. 2013; Normand et al. 2014; Corporeau et al. 2014; He et al. 2015). This
593 indicates a change in ROS balance and induction of oxidative stress as a response to the
594 infection, and also suggests that the ROS-regulatory system is an important feature which
595 underpins disease resistance.

596 We detected a relatively high coverage of metabolites within the glutathione
597 metabolism pathway. However, subtle variations of metabolites central to network topology,
598 such as glutathione itself, were not differentially expressed resulting in the entire pathway
599 being only marginally affected ($p = 0.057$). On the other hand, the transulphuration pathway
600 (cysteine and methionine metabolism) which is responsible for supplying precursor
601 metabolites for glutathione synthesis under low-mid stress conditions was altered, which
602 indicates a mild oxidative stress response. The subtle signs of oxidative stress and perturbed
603 redox balance in virus-exposed larvae indicate that the homeostatic control mechanisms
604 responsible for governing the production and detoxification of ROS were functioning at
605 optimal capacities and well within acceptable boundaries. These findings suggest that OsHV-
606 1 either does not induce major oxidative stress in oyster larvae beyond the adaptive ability of
607 the ROS-regulatory system, or that the level or stage of infection in our study was low or
608 early, respectively. These results also may highlight a potential limitation in the exclusive use
609 of metabolomic-based approaches to recognise changes in metabolic activity under
610 circumstances where enzymatic regulation tightly constrains metabolite levels within the
611 range of normal baseline variations. Indeed, cellular metabolism, and glutathione turnover/
612 ROS regulation in particular, is extremely well-adapted to achieve this feat. Thus, to better

613 define the influence of OsHV-1 on oxidative stress parameters, further analysis of enzymes
614 associated with glutathione recycling and ROS regulation would be required.

615 **4.5 Other signatures**

616 A number of other metabolites were considered to be important features responsible for larval
617 health class discrimination in PCA, PLS-DA and RF models. These included elevated levels
618 of 4-hydroxyphenylacetic acid, 4-hydroxyproline, and 2-aminoadipic acid and a reduction in
619 nicotinic acid contents. Four unannotated metabolites were also important in the multivariate
620 models. Future efforts to identify these molecules may further complement our interpretations
621 or provide new insights into the virus-host interaction.

622 4-hydroxyphenylacetic acid (4-HPA) is a tyrosine-derived metabolite with antioxidant
623 activity that can scavenge reactive oxygen and nitrogen species *in vitro* and *in vivo* (Biskup et
624 al. 2013), and also has an ability to reduce excessive release of proinflammatory cytokines
625 which protects against inflammation and disease (Liu et al. 2014; Ford et al. 2016). Increased
626 levels of 4-HPA are associated with various mammalian disease pathologies and inborn
627 errors in metabolism (Kikuchi et al. 2010; Nishiumi et al. 2010; Hori et al. 2011; Manna et al.
628 2015; Xiong et al. 2015; Kurko et al. 2016). An accumulation of this metabolite during such
629 disease onsets has been attributed to differential catabolic pathways of tyrosine (Xiong et al.
630 2015). In our study, tyrosine metabolism was identified as a pathway with signs of being
631 differentially regulated. It was recently demonstrated that the mechanism by which 4-HPA
632 reduces proinflammatory cytokine production involves suppression of their transcription via
633 promotion of HIF-1α protein degradation (Liu et al. 2014). Thus, with a functional role in
634 downregulating HIF-1 activity, 4-HPA could directly compete with *Irg1*/ITA/succinic acid-
635 induced HIF-1α stabilisation. As a result, HIF-1 induced enrichment of pathways responsible
636 for redirecting carbon and nitrogen metabolism in trajectories which support OsHV-1

637 proliferation might be moderated, whereas the negative host consequences associated with
638 co-induced respiratory dysfunction and excessive inflammation may partially be alleviated.
639 4-hydroxyproline (4-HP) is produced via the posttranslational hydroxylation of
640 proline and is formed in proteins only after peptide linkage (Cooper et al. 2008). 4-HP is
641 predominantly found in collagen, a major structural component of the extracellular matrix
642 (ECM) scaffold in marine invertebrate embryos and larvae (Spiegel et al. 1989; Phang et al.
643 2010). Thus, accumulation of free 4-HP is a specific biomarker of collagen degradation, and
644 indicator of cell structure damage through compositional transformation of the ECM (Karna
645 & Palka 2002; Phang et al. 2008). The production of free 4-HP resulting from ECM
646 degradation is thought to play a role in initiating the apoptotic cascade via activation of the
647 caspase-9 protease (Cooper et al. 2008), as well as promoting HIF-1 activity by inhibiting the
648 degradation of HIF-1α (Surazynski et al. 2008). Matrix metalloproteinases (MMPs), are
649 responsible for degrading the ECM. MMPs play crucial roles during normal embryonic and
650 larval development, such as in cell growth and differentiation, tissue remodelling, and
651 mechanisms of immunological defense (Mannello et al. 2003, 2005; Mok et al. 2009).
652 However, MMPs can be excessively produced in pathological situations (Itoh et al. 2006;
653 Phang et al. 2008). Physical stress, oncogenic transformation, ROS and cytokines are all
654 inducible factors (Mancini & Battista 2006; Reuter et al. 2010). MMPs and their importance
655 in restructuring the ECM as a response to pathogens have previously been implicated in
656 OsHV-1 infections and disease resistance vs susceptibility traits of oysters (McDowell et al.
657 2014; Nikapitiya et al. 2014; Rosani et al. 2015). The elevated levels of free 4-HP in OsHV-1
658 µVar-exposed larvae indicates that collagen degradation in the ECM was enhanced, although
659 further investigation will be required to determine whether the 4-HP accumulations represent
660 negative consequences for the host due to significant cell structure damage.

2-aminoadipic acid (2-AAA) is a component of the lysine metabolism pathway and is recognised as a small-molecule biomarker of oxidative stress (Sell et al. 2007; Zeitoun-Ghandour et al. 2011). Its presence has been linked with regulation of glucose homeostasis (Yuan et al. 2011; Wang et al. 2013), and elevated levels have been reported as a putative biosignature of respiration chain disorders (Smuts et al. 2013). Production of 2-AAA in fish is associated with low oxygen transport capacity (Allen et al. 2015), and can be induced in shellfish by exposure to physiological stressors (Chen et al. 2015; Koyama et al. 2015). Accumulations of 2-AAA are also associated with oncogene activation and carcinogenesis, leading to its recent candidacy as a potential new clinical biomarker for various cancers (Hori et al. 2011; Bellance et al. 2012; Jung et al. 2013; Rosi et al. 2015; Ren et al. 2016). Production of 2-AAA correlates with the bioenergetic signature characteristic of a switch in cellular respiration modes from OxPhos to aerobic glucose fermentation (Hori et al. 2011; Aa et al. 2012; Bellance et al. 2012). Thus, the accumulation of 2-AAA in virus-exposed larvae is consistent with the global changes we detected in organic acid metabolism reflective of TCA cycle reprogramming, reduced mitochondrial respiration and ATP production, activation of the Warburg effect, and subtle signs of oxidative stress.

Nicotinic acid (NA) plays an important role in redox reactions and can be converted to nicotinamide (NAM) *in vivo*. In invertebrates and some fish, NA and NAM are important precursors for synthesis of the pyrimidine nucleotide coenzymes NAD^+ and $NADP^+$ which participate in many hydrogen transfer processes, such as fatty acid synthesis, lipolysis and glycolysis (Ng et al. 1997; Sauve 2008; Houtkooper et al. 2009; Cantó et al. 2015; Yuasa & Ball 2015; Yuasa et al. 2015). NAD^+ is also a substrate and signalling metabolite required for regulation of transcription, proteasomal function, and posttranslational protein modifications involved in DNA replication, recombination, repair mechanisms and maintenance of genomic stability (Bürkle 2001; Surjana et al. 2010; Vyas et al. 2013; Fouquerel & Sobol 2014; Cantó

686 et al. 2015). Unlike most metabolic redox reactions which reversibly oxidise or reduce
687 pyrimidine nucleotides to maintain constant levels of $NAD^+/NADP^+$, substrate utilisation and
688 NAD^+-dependant signalling processes are highly consumptive, and regeneration from niacin
689 precursors is required when such mechanisms are activated (Lin 2007; Chiarugi et al. 2012).
690 The reduction of free NA in virus-exposed larvae is consistent with its role in these processes
691 which are upregulated during herpes-type viral infections (Grady et al. 2012; Li et al. 2012).
692 Herpes-induced consumption of NAD^+ as a substrate for enzymes involved in host DNA
693 modifications is likely a response to DNA damage pathways being activated by replication of
694 the viral genome (Grady et al. 2012). However, efficient virus replication itself and synthesis
695 of viral proteins are also reliant on NAD^+ substrate supply (Li et al. 2012). Thus, the
696 importance of NA and $NAD^+/NADP^+$ metabolism in host-pathogen interactions is gaining
697 considerable attention as targets for the treatment of infectious diseases in humans (Mesquita
698 et al. 2016). Interestingly, activation of the Warburg effect involves the unusual
699 overproduction of NAD^+ via enhanced fermentation of glucose (i.e., pyruvic acid + NADH
700 $\rightarrow$ lactic acid + NAD^+) (Chiarugi et al. 2012), and may serve/function as a replenishing
701 mechanism in response to NAD^+ depletion to complement *de novo* synthesis from its niacin
702 precursors.

703 **4.6 Study limitations**

704 During an infection, viruses have an ability to alter host metabolites in order to benefit their
705 replication. However, the host can also mount responses against the pathogen via changes in
706 host metabolism pathways, such as triggering inflammation. Unfortunately, at this early stage
707 of the research we do not know which metabolic features have roles in virus pathogenesis and
708 which of the signatures can be attributed to host defence. This is an important aspect to
709 decipher, and will require highly focused investigation. A critical step to achieve this will be

710 to characterise the functional genome of OsHV-1 µVar. Furthermore, our study did not
711 include a temporal sampling design. During an infection, viruses can trigger various
712 metabolic changes at different replication stages. For example, the Warburg effect may be
713 triggered at the stage of virus genome replication, whereas lipid metabolism may be altered at
714 the stage of virion assembly prior to release of mature virion particles from host cells. In
715 order to contextualise host metabolic perturbations within the framework of viral
716 propagation, future efforts should be made to incorporate a fine scale temporal sampling
717 design, analysis of multiple targets (genes, proteins and metabolites), and a detailed
718 characterisation of the virus replication process; although, lack of bivalve cell lines continue
719 to hamper virus research in these taxa (Yoshino & Bayne 2013).

720 **5. CONCLUSION**

721 In summary, we identified and measured the metabolic responses of oyster larvae during
722 exposure to the virulent ostreid herpesvirus microvariant which has recently been responsible
723 for mass mortalities of shellfish around the globe. Viruses can reshape their host's
724 metabolism to create a unique metabolic state that supports their specific requirements.
725 Indeed, profiling of larval metabolites revealed virus-induced reprogramming of host-
726 encoded metabolic networks, including alterations to the glycolytic pathway, the TCA cycle,
727 and lipid metabolism. Intriguingly, we observed metabolic response parallels with a number
728 of innate immune system mechanisms previously characterised in mammalian cell models,
729 such as induction of the Warburg effect and downstream metabolic consequences of
730 immunoresponsive gene 1 like activation. The functional genomes of OsHV-1 and its
731 variants are mostly unknown at present, but it is likely that virus-encoded auxiliary genes also
732 provide infected host cells with novel metabolic capabilities, and the outcomes of their
733 transcription may be manifested within our results. These findings provide the first

734 comprehensive insights into early ontogenic host physiology and susceptibility of oysters
735 towards OsHV-1 µVar. Characterisation of host-virus interactions can provide knowledge to
736 enable development of therapeutic agents and identify traits for improving the outcome of
737 selective breeding programmes. Our study also highlights the value of metabolomics-based
738 approaches in elucidating host-virus interactions and the metabolic networks which
739 characterise and underpin the pathophysiological state, and further supports its application for
740 investigating pathogenesis of disease in early life stage oyster models.

741 **ACKNOWLEDGEMENTS**

742 We would like to thank the crew at the Cawthron Aquaculture Park for their support and
743 guidance: Norman Ragg, Serean Adams, Zoë Hilton, Steve Webb, Samantha Gale, Henry
744 Kaspar, and Mark Camara. We are thankful to the Aquaculture Biotechnology Group (AUT)
745 for their input and support through this research. We are also thankful to Francesca Casu and
746 Erica Zarate from University of Auckland for their technical assistance with sample analysis.
747 We acknowledge support from an Auckland University of Technology Vice Chancellor
748 Doctoral Scholarship to T. Young under the supervision of A.C. Alfaro. This work was
749 funded by the New Zealand Ministry of Business, Innovation and Employment (CAWX0802
750 and CAWX1315).

751 **REFERENCES**

752

753 Aa, J., Yu, L., Sun, M., Liu, L., Li, M., Cao, B., et al., 2012. Metabolic features of the tumor
754 microenvironment of gastric cancer and the link to the systemic macroenvironment.
755 Metabolomics, 8(1), 164–173.

756 Alfaro, A.C., Young, T., 2016. Showcasing metabolomics research in aquaculture: A review.
757 Rev. Aquacult., DOI: 10.1111/raq.12152

758 Allen, P.J., Wise, D., Greenway, T., Khoo, L., Griffin, M.J., Jablonsky, M., 2015. Using 1-D
759 ^{1}H and 2-D ^{1}H J-resolved NMR metabolomics to understand the effects of anemia in
760 channel catfish (*Ictalurus punctatus*). Metabolomics, 11(5), 1131–1143.

761 Apel, K., Hirt, H., 2004. Reactive oxygen species: Metabolism, oxidative stress, and signal
762 transduction. Annu. Rev. Plant Biol., 55, 373–399.

763 Arzul, I., Nicolas, J.-L., Davison, A.J., Renault, T., 2001. French scallops: A new host for
764 ostreid herpesvirus-1. Virology, 290, 342–349.

765 Azéma P., Travers, M.A., Benabdelmouna, A., Dégremont, L., 2016. Single or dual
766 experimental infections with *Vibrio aestuarianus* and OsHV-1 in diploid and triploid
767 *Crassostrea gigas* at the spat, juvenile and adult stages. J. Invertebr. Pathol., 139, 92–
768 101.

769 Bai, C., Gao, W., Wang, C., Yu, T., Zhang, T., Qiu, Z., et al., 2016. Identification and
770 characterization of ostreid herpesvirus 1 associated with massive mortalities of
771 *Scapharca broughtonii* broodstocks in China. Dis. Aquat. Organ., 118(1), 65–75.

772 Bai, C., Wang, C., Xia, J., Sun, H., Zhang, S., Huang, J., 2015. Emerging and endemic types
773 of Ostreid herpesvirus 1 were detected in bivalves in China. J. Invertebr. Pathol., 124,
774 98–106.

775 Barnard, R., 2014. Determining the Need for a Multi-Species Mollusc Hatchery in Western
776 Australia: ACWA Study Report. Australian Community Workers Association Mollusc
777 Hatchery Report prepared by RMB Aqua, Albany, WA, Australia.

778 Batista, F.M., López-Sanmartín, M., Grade, A., Morgado, I., Valente, M., Navas, J.I., et al.,
779 2015. Sequence variation in ostreid herpesvirus 1 microvar isolates detected in dying and
780 asymptomatic *Crassostrea angulata* adults in the Iberian Peninsula: Insights into viral
781 origin and spread. Aquaculture, 435, 43–51.

782 Bellance, N., Pabst, L., Allen, G., Rossignol, R., Nagrath, D., 2012. Oncosecretomics coupled
783 to bioenergetics identifies α-amino adipic acid, isoleucine and GABA as potential
784 biomarkers of cancer: Differential expression of c-Myc, Oct1 and KLF4 coordinates
785 metabolic changes. BBA-Bioenergetics, 1817(11), 2060–2071.

786 Ben-Shlomo, I., Kol, S., Roeder, L.M., Resnick, C.E., Hurwitz, A., Payne, D.W., et al., 1997.
787 Interleukin (IL)-1β increases glucose uptake and induces glycolysis in aerobically
788 cultured rat ovarian cells: Evidence that IL-1β may mediate the gonadotropin-induced
789 midcycle metabolic shift. Endocrinology, 138(7), 2680–2688.

790 Bhatt, A.P., Jacobs, S.R., Freemerman, A.J., Makowski, L., Rathmell, J.C., Dittmer, D.P., et
791 al., 2012. Dysregulation of fatty acid synthesis and glycolysis in non-Hodgkin
792 lymphoma. P. Natl. Acad. Sci. U. S. A., 109(29), 11818–11823.

793 Biskup, I., Golonka, I., Gamian, A., Sroka, Z., 2013. Antioxidant activity of selected phenols
794 estimated by ABTS and FRAP methods. Postep. Hig. Med. Dosw., 67, 958–963.

795 Bouhifd, M., Hartung, T., Hogberg, H.T., Kleensang, A., Zhao, L., 2013. Review:
796 Toxicometabolomics. J. Appl. Toxicol., 33(12), 1365–1383.

797 Braundmeier-Fleming, A., Russell, N.T., Yang, W., Nas, M.Y., Yaggie, R.E., Berry, M., et
798 al., 2016. Stool-based biomarkers of interstitial cystitis/bladder pain syndrome. Sci. Rep.,
799 DOI: 10.1038/srep26083

800 Burge, C.A., Griffin, F.J., Friedman, C.S., 2006. Mortality and herpesvirus infections of the
801 Pacific oyster *Crassostrea gigas* in Tomales Bay, California, USA. Dis. Aquat. Organ.,
802 72(1), 31–43.

803 Burge, C., Judah, L.R., Conquest, L.L., Griffin, F.J., Cheney, D.P., Suhrbier, A., et al., 2007.
804 Summer seed mortality of the Pacific oyster, *Crassostrea gigas* Thunberg grown in
805 Tomales Bay, California, U. S. A.: The influence of oyster stock, planting time,
806 pathogens, and environmental stressors. J. Shellfish Res., 26, 163–172.

807 Burge, C.A., Strenge, R.E., Friedman, C.S., 2011. Detection of the oyster herpesvirus in
808 commercial bivalves in northern California, USA: Conventional and quantitative PCR.
809 Dis. Aquat. Organ., 94(2), 107–116.

810 Burge, C.A., Friedman, C.S., 2012. Quantifying ostreid herpesvirus (OsHV-1) genome copies
811 and expression during transmission. Microb. Ecol., 63(3), 596–604.

812 Burioli, E.A.V., Prearo, M., Riina, M.V., Bona, M.C., Fioravanti, M.L., Arcangeli, G., et al.,
813 2016. Ostreid herpesvirus type 1 genomic diversity in wild populations of Pacific oyster
814 *Crassostrea gigas* from Italian coasts. J. Invertebr. Pathol., 137, 71–83.

815 Bürkle, A., 2001. Physiology and pathophysiology of poly (ADP-ribosyl) ation. Bioessays,
816 23(9), 795–806.

817 Cameron, S.J., Lewis, K.E., Beckmann, M., Allison, G.G., Ghosal, R., Lewis, P.D., et al.,
818 2016. The metabolomic detection of lung cancer biomarkers in sputum. Lung Cancer, 94,
819 88–95.

820 Cantó, C., Menzies, K.J., Auwerx, J., 2015. NAD^+ metabolism and the control of energy
821 homeostasis: A balancing act between mitochondria and the nucleus. Cell Metab., 22(1),
822 31–53.

823 Cascante, M., Marin, S., 2008. Metabolomics and fluxomics approaches. Essays Biochem.,
824 45, 67–82.

825 Castinel, A, Fletcher, L, Dhand, N, Rubio, A, Whittington, R, Taylor, M., 2015. OsHV-1
826 mortalities in Pacific Oysters in Australia and New Zealand: The Farmer's Story.
827 Prepared for the Ministry of Business, Innovation and Employment (MBIE). Cawthron
828 Report No. 2567. 48 p.

829 Chambers, J.W., Maguire, T.G., Alwine, J.C., 2010. Glutamine metabolism is essential for
830 human cytomegalovirus infection. J. Virol., 84(4), 1867–1873.

831 Chen, D.Q., Chen, H., Chen, L., Tang, D.D., Miao, H., Zhao, Y.Y., 2016a. Metabolomic
832 application in toxicity evaluation and toxicological biomarker identification of natural
833 product. Chem.-Biol. Interact., 252, 114–130.

834 Chen, I.T., Lee, D.Y., Huang, Y.T., Kou, G.H., Wang, H.C., Chang, G.D., et al., 2016b. Six
835 hours after infection, the metabolic changes induced by WSSV neutralize the host's
836 oxidative stress defenses. Sci. Rep., 6, Article number 27732.

837 Chen, S., Zhang, C., Xiong, Y., Tian, X., Liu, C., Jeevithan, E. et al., 2015. A GC-MS-based
838 metabolomics investigation on scallop (*Chlamys farreri*) during semi-anhydrous living-
839 preservation. Innov. Food Sci. Emerg., 31, 185–195.

840 Chiang, E., Dang, O., Anderson, K., Matsuzawa, A., Ichijo, H., David, M., 2006. Cutting
841 edge: Apoptosis-regulating signal kinase 1 is required for reactive oxygen species-
842 mediated activation of IFN regulatory factor 3 by lipopolysaccharide. J. Immunol.,
843 176(10), 5720–5724.

844 Chiarugi, A., Dölle, C., Felici, R., Ziegler, M., 2012. The NAD metabolome – a key
845 determinant of cancer cell biology. Nat. Rev. Cancer, 12(11), 741–752.

846 Chukkapalli, V., Heaton, N.S., Randall, G., 2012. Lipids at the interface of virus–host
847 interactions. Curr. Opin. Microbiol., 15(4), 512–518.

848 Cooper, S.K., Pandhare, J., Donald, S.P., Phang, J.M., 2008. A novel function for
849 hydroxyproline oxidase in apoptosis through generation of reactive oxygen species. J.
850 Biol. Chem., 283(16), 10485–10492.

851 Cordes, T., Wallace, M., Michelucci, A., Divakaruni, A.S., Sapcariu, S.C., Sousa, C., et al.,
852 2016. Immunoresponsive gene 1 and itaconate inhibit succinate dehydrogenase to
853 modulate intracellular succinate levels. J. Biol. Chem., 291(27), 14274–14284.

854 Corporeau, C., Tamayo, D., Pernet, F., Quéré, C., Madec, S., 2014. Proteomic signatures of
855 the oyster metabolic response to herpesvirus OsHV-1 µVar infection. J. Proteomics, 109,
856 176–187.

857 Darekar, S., Georgiou, K., Yurchenko, M., Yenamandra, S.P., Chachami, G., Simos, G., et
858 al., 2012. Epstein-Barr virus immortalization of human B-cells leads to stabilization of
859 hypoxia-induced factor 1 alpha, congruent with the Warburg effect. PLOS ONE, 7(7),
860 e42072.

861 Davis, J., 2016. A National Industry Response to Pacific Oyster Mortality Syndrome
862 (POMS). An Agribusiness Tasmanian report commissioned by Oysters Australia Ltd,
863 Tasmania, Australia.

864 Davison, A.J., Trus, B.L., Cheng, N., Steven, A.C., Watson, M.S., Cunningham, C., et al.,
865 2005. A novel class of herpesvirus with bivalve hosts. J. Gen. Virol., 86(1), 41–53.

866 Dégremont, L., 2013. Size and genotype affect resistance to mortality caused by OsHV-1 in
867 *Crassostrea gigas*. Aquaculture, 416, 129–134.

868 Dégremont, L., Lamy, J.B., Pépin, J.F., Travers, M.A., Renault, T., 2015a. New insight for
869 the genetic evaluation of resistance to Ostreid herpesvirus infection, a worldwide disease,
870 in *Crassostrea gigas*. PLOS ONE, 10(6), e0127917.

871 Dégremont, L., Nourry, M., Maurouard, E., 2015b. Mass selection for survival and resistance
872 to OsHV-1 infection in *Crassostrea gigas* spat in field conditions: Response to selection
873 after four generations. Aquaculture, 446, 111–121.

874 Dégremont, L., Morga, B., Trancart, S., Pépin, J.F., 2016. Resistance to OsHV-1 infection in
875 *Crassostrea gigas* larvae. Front. Mar. Sci., 3, DOI: 10.3389/fmars.2016.00015

876 Delgado, T., Sanchez, E.L., Camarda, R., Lagunoff, M., 2012. Global metabolic profiling of
877 infection by an oncogenic virus: KSHV induces and requires lipogenesis for survival of
878 latent infection. PLOS Pathog., 8(8), e1002866.

879 DoA, 2015. AQUAVETPLAN disease strategy: Infection with ostreid herpesvirus-1
880 microvariant (Version 1), In: Australian Aquatic Veterinary Emergency Plan

(AQUAVETPLAN). Australian Government Department of Agriculture (DoA), Canberra, ACT, Australia.

Domeneghetti, S., Varotto, L., Civettini, M., Rosani, U., Stauder, M., Pretto, T., et al., 2014. Mortality occurrence and pathogen detection in *Crassostrea gigas* and *Mytilus galloprovincialis* close-growing in shallow waters (Goro lagoon, Italy). Fish Shellfish Immunol., 41(1), 37–44.

Ellis, R.P., Spicer, J.I., Byrne, J.J., Sommer, U., Viant, M.R., White, D.A., et al., 2014. ^{1}H NMR metabolomics reveals contrasting response by male and female mussels exposed to reduced seawater pH, increased temperature, and a pathogen. Environ. Sci. Technol., 48(12), 7044–7052.

Evans, O., Hick, P., Whittington, R.J., 2016. Distribution of Ostreid herpesvirus-1 (OsHV-1) microvariant in seawater in a recirculating aquaculture system. Aquaculture, 458, 21–28.

Fan, W., Ye, Y., Chen, Z., Shao, Y., Xie, X., Zhang, W., et al., 2016. Metabolic product response profiles of *Cherax quadricarinatus* towards white spot syndrome virus infection. Dev. Comp. Immunol., 61, 236–241.

FAO, 2016b. Global Aquaculture Production dataset (online query). http://www.fao.org/fishery/statistics/global-aquaculture-production/query/en (accessed 19.09.2016). Food and Agriculture Organisation of the United Nations (FAO), Fisheries and Aquaculture Department, Rome, Italy.

Ferreira, L.M., 2010. Cancer metabolism: The Warburg effect today. Exp. Mol. Pathol., 89(3), 372–380.

Feussner, I., Polle, A., 2015. What the transcriptome does not tell—proteomics and metabolomics are closer to the plants' patho-phenotype. Curr. Opin. Plant Biol., 26, 26–31.

Fiehn, O., 2002. Metabolomics – the link between genotypes and phenotypes. Plant Mol. Biol. Rep., 48(1–2), 155–171.

Fleury, E., Moal, J., Boulo, V., Daniel, J.Y., Mazurais, D., Hénaut, A., et al., 2010. Microarray-based identification of gonad transcripts differentially expressed between lines of Pacific oyster selected to be resistant or susceptible to summer mortality. Mar. Biotechnol., 12(3), 326–339.

Fleury, E., Huvet, A., 2012. Microarray analysis highlights immune response of Pacific oysters as a determinant of resistance to summer mortality. Mar. Biotechnol., 14(2), 203–217.

Ford, C.T., Richardson, S., McArdle, F., Lotito, S.B., Crozier, A., McArdle, A., et al., 2016. Identification of (poly) phenol treatments that modulate the release of pro-inflammatory cytokines by human lymphocytes. Br. J. Nutr., 115(10), 1699–1710.

Fouquerel, E., Sobol, R.W., 2014. ARTD1 (PARP1) activation and NAD^{+} in DNA repair and cell death. DNA Repair, 23, 27–32.

Friedman, C.S., Estes, R.M., Stokes, N.A., Burge, C.A., Hargove, J.S., Barber, B.J., et al., 2005. Herpes virus in juvenile Pacific oysters *Crassostrea gigas* from Tomales Bay, California, coincides with summer mortality episodes. Dis. Aquat. Organ., 63, 33–41.

Garcia, C., Thébault, A., Dégremont, L., Arzul, I., Miossec, L., Robert, M., et al., 2011. OsHV-1 detection and relationship with *C. gigas* spat mortality in France between 1998 and 2006. Vet. Res., 42, 73–84.

925 Gómez-Chiarri, M., Guo, X., Tanguy, A., He, Y., Proestou, D., 2015. The use of-omic tools
926 in the study of disease processes in marine bivalve mollusks. J. Invertebr. Pathol., 131,
927 137–154.

928 Goodwin, C.M., Xu, S., Munger, J., 2015. Stealing the keys to the kitchen: Viral
929 manipulation of the host cell metabolic network. Trends Microbiol., 23(12), 789–798.

930 Grady, S.L., Hwang, J., Vastag, L., Rabinowitz, J.D., Shenk, T., 2012. Herpes simplex virus
931 1 infection activates poly (ADP-ribose) polymerase and triggers the degradation of poly
932 (ADP-ribose) glycohydrolase. J. Virol., 86(15), 8259–8268.

933 Green, T.J., Robinson, N., Chataway, T., Benkendorff, K., O'Connor, W., Speck, P., 2014a.
934 Evidence that the major hemolymph protein of the Pacific oyster, *Crassostrea gigas*, has
935 antiviral activity against herpesviruses. Antiviral Res., 110, 168–174.

936 Green, T.J., Montagnani, C., Benkendorff, K., Robinson, N., Speck, P., 2014b. Ontogeny and
937 water temperature influences the antiviral response of the Pacific oyster, *Crassostrea*
938 *gigas*. Fish Shellfish Immunol., 36(1), 151–157.

939 Green, T.J., Rolland, J.L., Vergnes, A., Raftos, D., Montagnani, C., 2015. OsHV-1
940 countermeasures to the Pacific oyster's anti-viral response. Fish Shellfish Immunol.,
941 47(1), 435–443.

942 Grijalva-Chon, J.M., Castro-Longoria, R., Ramos-Paredes, J., Enríquez-Espinoza, T.L.,
943 Mendoza-Cano, F., 2013. Detection of a new OsHV-1 DNA strain in the healthy Pacific
944 oyster, *Crassostrea gigas* Thunberg, from the Gulf of California. J. Fish Dis., 36(11),
945 965–968.

946 He, Y., Jouaux, A., Ford, S.E., Lelong, C., Sourdaine, P., Mathieu, M., et al., 2015.
947 Transcriptome analysis reveals strong and complex antiviral response in a mollusc. Fish
948 Shellfish Immunol., 46(1), 131–144.

949 Hill, C.B., Taylor, J.D., Edwards, J., Mather, D., Langridge, P., Bacic, A., et al., 2015.
950 Detection of QTL for metabolic and agronomic traits in wheat with adjustments for
951 variation at genetic loci that affect plant phenology. Plant Sci., 233, 143–154.

952 Holmes, E., Wilson, I.D., Nicholson, J.K., 2008. Metabolic phenotyping in health and
953 disease. Cell, 134(5),714–717.

954 Hong, J., Yang, L., Zhang, D., Shi, J., 2016. Plant metabolomics: An indispensable system
955 biology tool for plant science. Int. J. Mol. Sci., 17(6), E767, DOI: 10.3390/ijms17060767

956 Hori, S., Nishiumi, S., Kobayashi, K., Shinohara, M., Hatakeyama, Y., Kotani, Y., et al.,
957 2011. A metabolomic approach to lung cancer. Lung Cancer, 74(2), 284–292.

958 Houtkooper, R.H., Cantó, C., Wanders, R.J., Auwerx, J., 2010. The secret life of NAD^+: An
959 old metabolite controlling new metabolic signaling pathways. Endocr. Rev., 31(2), 194–
960 223.

961 Hsieh, Y.C., Chen, Y.M., Li, C.Y., Chang, Y.H., Liang, S.Y., Lin, S.Y., et al., 2015. To
962 complete its replication cycle, a shrimp virus changes the population of long chain fatty
963 acids during infection via the PI3K-Akt-mTOR-HIF1α pathway. Dev. Comp. Immunol.,
964 53(1), 85–95.

965 Hwang, J.Y., Park, J.J., Yu, H.J., Hur, Y.B., Arzul, I., Couraleau, Y., et al., 2013. Ostreid
966 herpesvirus 1 infection in farmed Pacific oyster larvae *Crassostrea gigas* (Thunberg) in
967 Korea. J. Fish Dis., 36(11), 969–972.

Itoh, M., Murata, T., Suzuki, T., Shindoh, M., Nakajima, K., Imai, K., et al., 2006. Requirement of STAT3 activation for maximal collagenase-1 (MMP-1) induction by epidermal growth factor and malignant characteristics in T24 bladder cancer cells. Oncogene, 25(8), 1195–1204.

Jee, B.Y., Lee, S.J., Cho, M.Y., Lee, S.J., Kim, J.W., Choi, S.H., et al., 2013. Detection of ostreid herpesvirus 1 from adult Pacific oysters *Crassostrea gigas* cultured in Korea. J. Kor. Fish. Aqua. Sci., 16(2), 131–135.

Jenkins, C., Hick, P., Gabor, M., Spiers, Z., Fell, S.A., Gu, X., et al., 2013. Identification and characterisation of an ostreid herpesvirus-1 microvariant (OsHV-1 µ-var) in *Crassostrea gigas* (Pacific oysters) in Australia. Dis. Aquat. Organ., 105(2), 109–126.

Jha, A.K., Huang, S.C.C., Sergushichev, A., Lampropoulou, V., Ivanova, Y., Loginicheva, E., et al., 2015. Network integration of parallel metabolic and transcriptional data reveals metabolic modules that regulate macrophage polarization. Immunity, 42(3), 419–430.

Jung, K., Reszka, R., Kamlage, B., Bethan, B., Stephan, C., Lein, M., et al., 2013. Tissue metabolite profiling identifies differentiating and prognostic biomarkers for prostate carcinoma. Int. J. Cancer, 133(12), 2914–2924.

Kalantari, S., Nafar, M., Samavat, S., Parvin, M., Fatemeh, B., Barzi, F., 2016. ^{1}H NMR-based metabolomics exploring urinary biomarkers correlated with proteinuria in focal segmental glomerulosclerosis: A pilot study. Magn. Reson. Chem., 54(10), 821–826.

Kanehisa, M., Goto, S., 2000. KEGG: Kyoto Encyclopedia of Genes and Genomes. Nucleic Acids Res., 28, 27–30.

Karna, E., Pałka, J.A., 2002. Inhibitory effect of acetylsalicylic acid on metalloproteinase activity in human lung adenocarcinoma at different stages of differentiation. Eur. J. Pharmacol., 443(1), 1–6.

Karnovsky, A., Weymouth, T., Hull, T., Tarcea, V.G., Scardoni, G., Laudanna, C., et al., 2012. Metscape 2 bioinformatics tool for the analysis and visualization of metabolomics and gene expression data. Bioinformatics, 28(3), 373–380.

Keeling, S.E., Brosnahan, C.L., Williams, R., Gias, E., Hannah, M., Bueno, R., et al., 2014. New Zealand juvenile oyster mortality associated with ostreid herpesvirus 1—an opportunistic longitudinal study. Dis. Aquat. Organ., 109, 231–239.

Kelly, B., O'Neill, L.A., 2015. Metabolic reprogramming in macrophages and dendritic cells in innate immunity. Cell Res., 25(7), 771–784.

Kikuchi, K., Itoh, Y., Tateoka, R., Ezawa, A., Murakami, K., Niwa, T., 2010. Metabolomic analysis of uremic toxins by liquid chromatography/electrospray ionization-tandem mass spectrometry. J. Chromatogr. B Biomed. Sci. Appl., 878(20), 1662–1668.

Knight, J.A., 2000. Review: Free radicals, antioxidants, and the immune system. Ann. Clin. Lab. Sci., 30(2), 145–158.

Koyama, H., Okamoto, S., Watanabe, N., Hoshino, N., Jimbo, M., Yasumoto, K., et al., 2015. Dynamic changes in the accumulation of metabolites in brackish water clam *Corbicula japonica* associated with alternation of salinity. Comp. Biochem. Physiol. B Biochem. Mol. Biol., 181, 59–70.

1010 Koyuncu, E., Purdy, J.G., Rabinowitz, J.D., Shenk, T., 2013. Saturated very long chain fatty
1011 acids are required for the production of infectious human cytomegalovirus progeny.
1012 PLOS Pathog., 9(5), e1003333.

1013 Kurko, J., Tringham, M., Tanner, L., Näntö-Salonen, K., Vähä-Mäkilä, M., Nygren, H., et al.,
1014 2016. Imbalance of plasma amino acids, metabolites and lipids in patients with lysinuric
1015 protein intolerance (LPI). Metabolism, 65(9), 1361–1375.

1016 Lampropoulou, V., Sergushichev, A., Bambouskova, M., Nair, S., Vincent, E.E.,
1017 Loginicheva, E., et al., 2016. Itaconate links inhibition of succinate dehydrogenase with
1018 macrophage metabolic remodeling and regulation of inflammation. Cell Metab., 24(1),
1019 158–166.

1020 Lewis, T., Defenderfer, D., Zippel, B., 2012. Understanding and Planning for the Potential
1021 Impacts of OsHV-1 µVar on the Australian Pacific oyster Industry. Final report (FRDC
1022 2011/043), 1 September 2012. RDS Partners, Hobart, Australia, pp. 1–21.

1023 Li, C.Y., Wang, Y.J., Huang, S.W., Cheng, C.S., Wang, H.C., 2016. Replication of the
1024 shrimp virus WSSV depends on glutamate-driven anaplerosis. PLOS ONE, 11(1),
1025 e0146902.

1026 Li, Z., Yamauchi, Y., Kamakura, M., Murayama, T., Goshima, F., Kimura, H., et al., 2012.
1027 Herpes simplex virus requires poly (ADP-ribose) polymerase activity for efficient
1028 replication and induces extracellular signal-related kinase-dependent phosphorylation
1029 and ICP0-dependent nuclear localization of tankyrase 1. J. Virol., 86(1), 492–503.

1030 Lin, H., 2007. Nicotinamide adenine dinucleotide: beyond a redox coenzyme. Org. Biomol.
1031 Chem., 5(16), 2541–2554.

1032 Lionel, D., Guyader, T., Tourbiez, D., Pépin, J.F., 2013. Is horizontal transmission of the
1033 Ostreid herpesvirus OsHV-1 in *Crassostrea gigas* affected by unselected or selected
1034 survival status in adults to juveniles? Aquaculture, 408, 51–57.

1035 Littlewood-Evans, A., Sarret, S., Apfel, V., Loesle, P., Dawson, J., Zhang, J., et al., 2016.
1036 GPR91 senses extracellular succinate released from inflammatory macrophages and
1037 exacerbates rheumatoid arthritis. J. Exp. Med., 213(9), 1655–1662.

1038 Liu, P.F., Liu, Q.H., Wu, Y., Jie, H., 2015. A pilot metabolic profiling study in
1039 hepatopancreas of *Litopenaeus vannamei* with white spot syndrome virus based on ^{1}H
1040 NMR spectroscopy. J. Invertebr. Pathol., 124, 51–56.

1041 Liu, Z., Xi, R., Zhang, Z., Li, W., Liu, Y., Jin, F., et al., 2014. 4-Hydroxyphenylacetic acid
1042 attenuated inflammation and edema via suppressing HIF-1α in seawater aspiration-
1043 induced lung injury in rats. Int. J. Mol. Sci., 15(7), 12861–12884.

1044 Ma, Y.M., Yang, M.J., Wang, S., Li, H., Peng, X.X., 2015. Liver functional metabolomics
1045 discloses an action of L-leucine against *Streptococcus iniae* infection in tilapias. Fish
1046 Shellfish Immunol., 45(2), 414–421.

1047 Maldonado, E.N., Lemasters, J.J., 2012. Warburg revisited: Regulation of mitochondrial
1048 metabolism by voltage-dependent anion channels in cancer cells. J. Pharmacol. Exp.
1049 Ther., 342(3), 637–641.

1050 Mancini, A., di Battista, J.A., 2006. Transcriptional regulation of matrix metalloprotease gene
1051 expression in health and disease. Front. Biosci., 11, 423–446.

1052 Manna, S.K., Thompson, M.D., Gonzalez, F.J., 2015. Application of mass spectrometry-
1053 based metabolomics in identification of early noninvasive biomarkers of alcohol-induced

liver disease using mouse model, In: Biological Basis of Alcohol-Induced Cancer. Springer International Publishing AG, Switzerland, pp. 217–238.

Mannello, F., Canesi, L., Faimali, M., Piazza, V., Gallo, G., Geraci, S., 2003. Characterization of metalloproteinase-like activities in barnacle (*Balanus amphitrite*) nauplii. Comp. Biochem. Physiol. B Biochem. Mol. Biol., 135(1), 17–24.

Mannello, F., Tonti, G., Papa, S., 2005. Are matrix metalloproteinases the missing link. Invertebrate Surviv. J., 2(69), 69–74.

Martenot, C., Oden, E., Travaille, E., Malas, J.P., Houssin, M., 2010. Comparison of two real-time PCR methods for detection of ostreid herpesvirus 1 in the Pacific oyster *Crassostrea gigas*. J. Virol. Methods, 170(1), 86–89.

Martenot, C., Lethuillier, O., Fourour, S., Oden, E., Trancart, S., Travaillé, E., et al., 2015. Detection of undescribed ostreid herpesvirus 1 (OsHV-1) specimens from Pacific oyster, *Crassostrea gigas*. J. Invertebr. Pathol., 132, 182–189.

Martenot, C., Segarra, A., Baillon, L., Faury, N., Houssin, M., Renault, T., 2016. In situ localization and tissue distribution of ostreid herpesvirus 1 proteins in infected Pacific oyster, *Crassostrea gigas*. J. Invertebr. Pathol., 136, 124–135.

Martín-Gómez, L., Villalba, A., Abollo, E., 2012. Identification and expression of immune genes in the flat oyster *Ostrea edulis* in response to bonamiosis. Gene, 492(1), 81–93.

Mazzon, M., Mercer, J., 2014. Lipid interactions during virus entry and infection. Cell. Microbiol., 16(10), 1493–1502.

McDowell, I.C., Nikapitiya, C., Aguiar, D., Lane, C.E., Istrail, S., Gomez-Chiarri, M., 2014. Transcriptome of American oysters, *Crassostrea virginica*, in response to bacterial challenge: Insights into potential mechanisms of disease resistance. PLOS ONE, 9(8), e105097.

Meiser, J., Krämer, L., Sapcariu, S.C., Battello, N., Ghelfi, J., D'Herouel, A.F., et al., 2016. Pro-inflammatory macrophages sustain pyruvate oxidation through pyruvate dehydrogenase for the synthesis of itaconate and to enable cytokine expression. J. Biol. Chem., 291(8), 3932–3946.

Mesquita, I., Varela, P., Belinha, A., Gaifem, J., Laforge, M., Vergnes, B., et al., 2016. Exploring NAD^+ metabolism in host–pathogen interactions. Cell. Mol. Life Sci., 73(6), 1225–1236.

Mesri, E.A., Feitelson, M.A., Munger, K., 2014. Human viral oncogenesis: A cancer hallmarks analysis. Cell Host Microbe, 15(3), 266–282.

Michelucci, A., Cordes, T., Ghelfi, J., Pailot, A., Reiling, N., Goldmann, O., et al., 2013. Immune-responsive gene 1 protein links metabolism to immunity by catalyzing itaconic acid production. P. Natl. Acad. Sci. U. S. A., 110(19), 7820–7825.

Mills, E., O'Neill, L.A., 2014. Succinate: A metabolic signal in inflammation. Trends Cell Biol., 24(5), 313–320.

Mills, E.L., O'Neill, L.A., 2016. Reprogramming mitochondrial metabolism in macrophages as an anti-inflammatory signal. Eur. J. Immunol., 46(1), 13–21.

Milne, B., 2016. Outbreak of 'POMS' in Tasmanian hatchery offers new insight into ostreid herpesvirus. Hatchery Int., May 2016.

1096 Mineur, F., Provan, J., Arnott, G., 2015. Phylogeographical analyses of shellfish viruses:
1097 Inferring a geographical origin for ostreid herpesviruses OsHV-1 (Malacoherpesviridae).
1098 Mar. Biol., 162(1), 181–192.

1099 Mok, F.S., Thiyagarajan, V., Qian, P.Y., 2009. Proteomic analysis during larval development
1100 and metamorphosis of the spionid polychaete *Pseudopolydora vexillosa*. Proteome Sci.,
1101 7(1), 1–11.

1102 Mortensen, S., Strand, Å., Bodvin, T., Alfjorden, A., Skår, C.K., Jelmert, A., et al., 2016.
1103 Summer mortalities and detection of ostreid herpesvirus microvariant in Pacific oyster
1104 *Crassostrea gigas* in Sweden and Norway. Dis. Aquat. Organ., 117(3), 171–176.

1105 Munger, J., Bennett, B.D., Parikh, A., Feng, X.J., McArdle, J., Rabitz H.A., et al., 2008.
1106 Systems-level metabolic flux profiling identifies fatty acid synthesis as a target for
1107 antiviral therapy. Nat. Biotechnol., 26(10), 1179–1186.

1108 Naujoks, J., Tabeling, C., Dill, B.D., Hoffmann, C., Brown, A.S., Kunze, M., et al., 2016.
1109 IFNs modify the proteome of legionella-containing vacuoles and restrict infection via
1110 IRG1-derived itaconic acid. PLOS Pathog., 12(2), e1005408.

1111 Németh, B., Doczi, J., Csete, D., Kacso, G., Ravasz, D., Adams, D., et al., 2016. Abolition of
1112 mitochondrial substrate-level phosphorylation by itaconic acid produced by LPS-
1113 induced Irg1 expression in cells of murine macrophage lineage. FASEB J., 30(1), 286–
1114 300.

1115 Ng, W.K., Serrini, G., Zhang, Z., Wilson, R.P., 1997. Niacin requirement and inability of
1116 tryptophan to act as a precursor of NAD^+ in channel catfish, *Ictalurus punctatus*.
1117 Aquaculture, 152(1), 273–285.

1118 Nikapitiya, C., McDowell, I.C., Villamil, L., Muñoz, P., Sohn, S., Gomez-Chiarri, M., 2014.
1119 Identification of potential general markers of disease resistance in American oysters,
1120 *Crassostrea virginica* through gene expression studies. Fish Shellfish Immunol., 41(1),
1121 27–36.

1122 Nikiforova, V.J., Willmitzer, L., 2007. Network visualization and network analysis, in:
1123 Baginsky, S., Fernie, A.R. (Eds.), Plant Systems Biology. Birkhäuser Verlag, Basel,
1124 Switerland, pp. 245–275..

1125 Nishiumi, S., Shinohara, M., Ikeda, A., Yoshie, T., Hatan, N., Kakuyama, S., et al., 2010.
1126 Serum metabolomics as a novel diagnostic approach for pancreatic cancer.
1127 Metabolomics, 6(4), 518–528.

1128 Normand, J., Li, R., Quillien, V., Nicolas, J.L., Boudry, P., Pernet, F., et al., 2014. Contrasted
1129 survival under field or controlled conditions displays associations between mRNA levels
1130 of candidate genes and response to OsHV-1 infection in the Pacific oyster *Crassostrea*
1131 *gigas*. Mar. Genomics, 15, 95–102.

1132 O'Neill, L.A., 2015. A broken krebs cycle in macrophages. Immunity, 42(3), 393–394.

1133 O'Neill, L.A., Pearce, E.J., 2016. Immunometabolism governs dendritic cell and
1134 macrophage function. J. Exp. Med., 213(1), 15–23.

1135 O'Neill, L.A., Kishton, R.J., Rathmell, J., 2016. A guide to immunometabolism for
1136 immunologists. Nat. Rev. Immunol., 16, 553–565.

1137 Oden, E., Martenot, C., Berthaux, M., Travaillé, E., Malas, J.P., Houssin, M., 2011.
1138 Quantification of ostreid herpesvirus 1 (OsHV-1) in *Crassostrea gigas* by real-time PCR:

1139 determination of a viral load threshold to prevent summer mortalities. Aquaculture,
1140 317(1), 27–31.

1141 OIE, 2016. Infection with ostreid herpesvirus 1 microvariants, In: Manual of Diagnostic Tests
1142 for Aquatic Animals. World Organisation for Animal Health (OIE), Paris, France.

1143 Owens, L., Malham, S., 2015. Review of the RNA interference pathway in molluscs
1144 including some possibilities for use in bivalves in aquaculture. J. Mar. Sci. Eng., 3(1),
1145 87–99.

1146 Pallares-Méndez, R., Aguilar-Salinas, C.A., Cruz-Bautista, I., del Bosque-Plata, L., 2016.
1147 Metabolomics in diabetes, a review. Ann. Med., 48(1–2), 89–102.

1148 Palsson-McDermott, E.M., O'neill, L.A., 2013. The Warburg effect then and now: From
1149 cancer to inflammatory diseases. Bioessays, 35(11), 965–973.

1150 Paul-Pont, I., Dhand, N.K., Whittington, R.J., 2013. Influence of husbandry practices on
1151 OsHV-1 associated mortality of Pacific oysters *Crassostrea gigas*. Aquaculture, 412,
1152 202–214.

1153 Paul-Pont, I., Evans, O., Dhand, N.K., Whittington, R.J., 2015. Experimental infections of
1154 Pacific oyster *Crassostrea gigas* using the Australian OsHV-1 µVar strain. Dis. Aquat.
1155 Organ., 113(2), 137–147.

1156 Pernet, F., Barret, J., Marty, C., Moal, J., Le Gall, P., Boudry, P., 2010. Environmental
1157 anomalies, energetic reserves and fatty acid modifications in oysters coincide with an
1158 exceptional mortality event. Mar. Ecol. Prog. Ser., 401,129–46.

1159 Pernet, F., Lagarde, F., Jeannée, N., Daigle, G., Barret, J., Le Gall, P., et al., 2014. Spatial and
1160 temporal dynamics of mass mortalities in oysters is influenced by energetic reserves and
1161 food quality. PLOS ONE, 9, e88469.

1162 Petton, B., Pernet, F., Robert, R., Boudry, P., 2013. Temperature influence on pathogen
1163 transmission and subsequent mortalities in juvenile Pacific oysters *Crassostrea gigas*.
1164 Aquacult. Env. Interac., 3, 257–273.

1165 Phang, J.M., Donald, S.P., Pandhare, J., Liu, Y., 2008. The metabolism of proline, a stress
1166 substrate, modulates carcinogenic pathways. Amino Acids, 35(4), 681–690.

1167 Phang, J.M., Liu, W., Zabirnyk, O., 2010. Proline metabolism and microenvironmental stress.
1168 Annu. Rev. Nutr., 30, 441–463.

1169 Pisoschi, A.M., Pop, A., 2015. The role of antioxidants in the chemistry of oxidative stress: A
1170 review. Eur. J. Med. Chem., 97, 55–74.

1171 Preusse, M., Tantawy, M.A., Klawonn, F., Schughart, K., Pessler, F., 2013. Infection-and
1172 procedure-dependent effects on pulmonary gene expression in the early phase of
1173 influenza A virus infection in mice. BMC Microbiol., 13(1), 293, DOI: 10.1186/1471-
1174 2180-13-293

1175 Purdy, J.G., Shenk, T., Rabinowitz, J.D., 2015. Fatty Acid elongase 7 catalyzes lipidome
1176 remodeling essential for human cytomegalovirus replication. Cell Rep., 10(8), 1375–
1177 1385.

1178 Ragg, N.L., King, N., Watts, E., Morrish, J., 2010. Optimising the delivery of the key dietary
1179 diatom *Chaetoceros calcitrans* to intensively cultured Greenshell™ mussel larvae, *Perna*
1180 *canaliculus*. Aquaculture, 306(1), 270–280.

1181 Ren, S., Shao, Y., Zhao, X., Hong, C.S., Wang, F., Lu, X., et al., 2016. Integration of
1182 metabolomics and transcriptomics reveals major metabolic pathways and potential
1183 biomarker involved in prostate cancer. Mol. Cell. Proteomics, 15(1), 154–163.

1184 Ren, W., Chen, H., Renault, T., Cai, Y., Bai, C., Wang, C., et al., 2013. Complete genome
1185 sequence of acute viral necrosis virus associated with massive mortality outbreaks in the
1186 Chinese scallop, *Chlamys farreri*. Virol. J., 10(1), 110, DOI: 10.1186/1743-422X-10-110

1187 Renault, T., Le Deuff, R.M., Cochennec, N., Chollet, B., Maffart, P., 1995. Herpes-like
1188 viruses associated with high mortality levels in larvae and spat of Pacific oysters,
1189 *Crassostrea gigas*: A comparative study, the thermal effects on virus detection in
1190 hatchery-reared larvae, reproduction of the disease in axenic larvae. Vet. Res., 26(5–6),
1191 539–43.

1192 Renault, T., Arzul, I., 2001. Herpes-like virus infections in hatchery-reared bivalve larvae in
1193 Europe: Specific viral DNA detection by PCR. J. Fish Dis., 24(3), 161–168.

1194 Renault, T., Faury, N., Barbosa-Solomieu, V., Moreau, K., 2011. Suppression substractive
1195 hybridisation (SSH) and real time PCR reveal differential gene expression in the Pacific
1196 cupped oyster, *Crassostrea gigas*, challenged with Ostreid herpesvirus 1. Dev. Comp.
1197 Immunol., 35(7), 725–735.

1198 Renault, T., Moreau, P., Faury, N., Pepin, J.F., Segarra, A., Webb, S., 2012. Analysis of
1199 clinical Ostreid herpesvirus 1 (Malacoherpesviridae) specimens by sequencing amplified
1200 fragments from three virus genome areas. J. Virol., 86(10), 5942–5947.

1201 Renault, T., Tchaleu, G., Faury, N., Moreau, P., Segarra, A., Barbosa-Solomieu, V., et al.,
1202 2014. Genotyping of a microsatellite locus to differentiate clinical Ostreid herpesvirus 1
1203 specimens. Vet. Res., 45(1), 1–8.

1204 Reuter, S., Gupta, S.C., Chaturvedi, M.M., Aggarwal, B.B., 2010. Oxidative stress,
1205 inflammation, and cancer: How are they linked? Free Radic. Biol. Med., 49(11), 1603–
1206 1616.

1207 Rosani, U., Varotto, L., Domeneghetti, S., Arcangeli, G., Pallavicini, A., Venier, P., 2015.
1208 Dual analysis of host and pathogen transcriptomes in ostreid herpesvirus 1-positive
1209 *Crassostrea gigas*. Environ. Microbiol., 17(11), 4200–4212.

1210 Rosenwasser, S., Ziv, C., van Creveld, S.G., Vardi, A., 2016. Virocell metabolism: Metabolic
1211 innovations during host–virus interactions in the ocean. Trends Microbiol., 24(10), 821–
1212 832.

1213 Rosi, A., Ricci-Vitiani, L., Biffoni, M., Grande, S., Luciani, A.M., Palma, A., et al., 2015. ^{1}H
1214 NMR spectroscopy of glioblastoma stem-like cells identifies alpha-aminoadipate as a
1215 marker of tumor aggressiveness. NMR Biomed., 28(3), 317–326.

1216 Rubic, T., Lametschwandtner, G., Jost, S., Hinteregger, S., Kund, J., Carballido-Perrig, N., et
1217 al., 2008. Triggering the succinate receptor GPR91 on dendritic cells enhances
1218 immunity. Nat. Immunol., 9(11), 1261–1269.

1219 Sanchez, E.L., Carroll, P.A., Thalhofer, A.B., Lagunoff, M., 2015. Latent KSHV infected
1220 endothelial cells are glutamine addicted and require glutaminolysis for survival. PLOS
1221 Pathog., 11(7), e1005052.

1222 Sanchez, E.L., Lagunoff, M., 2015. Viral activation of cellular metabolism. Virology, 479,
1223 609–618.

Sanmartín, M.L., Power, D.M., de la Herrán, R., Navas, J.I., Batista, F.M., 2016. Experimental infection of European flat oyster *Ostrea edulis* with ostreid herpesvirus 1 microvar (OsHV-1µvar): Mortality, viral load and detection of viral transcripts by in situ hybridization. Virus Res., 217, 55–62.

Sauve, A.A., 2008. NAD^+ and vitamin B3: From metabolism to therapies. J. Pharmacol. Exp. Ther., 324(3), 883–893.

Schikorski, D., Faury, N., Pépin, J.F., Saulnier, D., Tourbiez, D., Renault, T., 2011a. Experimental ostreid herpesvirus 1 infection of the Pacific oyster *Crassostrea gigas*: Kinetics of virus DNA detection by q-PCR in seawater and in oyster samples. Virus Res., 155, 28–34.

Schikorski, D., Renault, T., Saulnier, D., Faury, N., Moreau, P., Pépin, J.F., 2011b. Experimental infection of Pacific oyster Crassostrea gigas spat by ostreid herpesvirus 1: Demonstration of oyster spat susceptibility. Vet. Res., 42(1), 27, DOI: 10.1186/1297-9716-42-27

Schmitt, P., Santini, A., Vergnes, A., Degremont, L., de Lorgeril, J., 2013. Sequence polymorphism and expression variability of *Crassostrea gigas* immune related genes discriminate two oyster lines contrasted in term of resistance to summer mortalities. PLOS ONE, 8(9), e75900.

Segarra, A., Pépin, J.F., Arzul, I., Morga, B., Faury, N., Renault, T., 2010. Detection and description of a particular Ostreid herpesvirus 1 genotype associated with massive mortality outbreaks of Pacific oysters, *Crassostrea gigas*, in France in 2008. Virus Res., 153(1), 92–99.

Segarra, A., Baillon, L., Tourbiez, D., Benabdelmouna, A., Faury, N., Bourgougnon, N., et al., 2014a. Ostreid herpesvirus type 1 replication and host response in adult Pacific oysters, *Crassostrea gigas*. Vet. Res., 45(1), 103, DOI: 10.1186/s13567-014-0103-x

Segarra, A., Mauduit, F., Faury, N., Trancart, S., Dégremont, L., Tourbiez, D., et al., 2014b. Dual transcriptomics of virus-host interactions: Comparing two Pacific oyster families presenting contrasted susceptibility to ostreid herpesvirus 1. *BMC Genomics*, 15(1), 580.

Segarra, A., Baillon, L., Faury, N., Tourbiez, D., Renault, T., 2016. Detection and distribution of ostreid herpesvirus 1 in experimentally infected Pacific oyster spat. J. Invertebr. Pathol., 133, 59–65.

Selak, M.A., Armour, S.M., MacKenzie, E.D., Boulahbel, H., Watson, D.G., Mansfield, K.D., et al., 2005. Succinate links TCA cycle dysfunction to oncogenesis by inhibiting HIF-α prolyl hydroxylase. Cancer Cell, 7(1), 77–85.

Sell, D.R., Strauch, C.M., Shen, W., Monnier, V.M., 2007. 2-Aminoadipic acid is a marker of protein carbonyl oxidation in the aging human skin: Effects of diabetes, renal failure and sepsis. Biochem J., 404(2), 269–277.

Semenza, G.L., 2010. HIF-1: Upstream and downstream of cancer metabolism. Curr. Opin. Genet. Dev., 20(1), 51–56.

Senyilmaz, D., Teleman, A.A., 2015. Chicken or the egg: Warburg effect and mitochondrial dysfunction. F1000Prime Rep., 7: 41, DOI: 10.12703/P7-41

Seo, J.Y., Cresswell, P., 2013. Viperin regulates cellular lipid metabolism during human cytomegalovirus infection. PLOS Pathog., 9(8), e1003497.

1267 Sévin, D.C., Kuehne, A., Zamboni, N., Sauer, U., 2015. Biological insights through
1268 nontargeted metabolomics. Curr. Opin. Biotechnol., 34, 1–8.

1269 Shannon, P., Markiel, A., Ozier, O., Baliga, N.S., Wang, J.T., Ramage, D., et al., 2003.
1270 Cytoscape: A software environment for integrated models of biomolecular interaction
1271 networks. Genome Res., 13(11), 2498–504.

1272 Shimahara, Y., Kurita, J., Kiryu, I., Nishioka, T., Yuasa, K., Kawana, M., et al., 2012.
1273 Surveillance of type 1 ostreid herpesvirus (OsHV-1) variants in Japan. Fish Pathol.,
1274 47(4), 129–136.

1275 Villas-Bôas, S.G., Smart, K.F., Sivakumaran, S., Lane, G.A., 2011. Alkylation or silylation
1276 for analysis of amino and non-amino organic acids by GC-MS?. *Metabolites*, 1(1), 3–20.

1277 Smuts, I., Van der Westhuizen, F.H., Louw, R., Mienie, L.J., Engelke, U.F., Wevers, R.A., et
1278 al., 2013. Disclosure of a putative biosignature for respiratory chain disorders through a
1279 metabolomics approach. *Metabolomics*, 9(2), 379–391.

1280 Spencer, C.M., Schafer, X.L., Moorman, N.J., Munger, J., 2011. Human cytomegalovirus
1281 induces the activity and expression of acetyl-coenzyme A carboxylase, a fatty acid
1282 biosynthetic enzyme whose inhibition attenuates viral replication. J. Virol., 85(12),
1283 5814–5824.

1284 Spiegel, E., Howard, L., Spiegel, M., 1989. Extracellular matrix of sea urchin and other
1285 marine invertebrate embryos. J. Morphol., 199(1), 71–92.

1286 Stehbens, W.E., 2004. Oxidative stress in viral hepatitis and AIDS. Exp. Mol. Pathol., 77(2),
1287 121–132.

1288 Størseth, T.R., Hammer, K.M., 2014. Environmental metabolomics of aquatic organisms.
1289 eMagRes, 2(4), DOI: 10.1002/9780470034590

1290 Su, M.A., Huang, Y.T., Chen, I.T., Lee, D.Y., Hsieh, Y.C., Li, C.Y., et al., 2014. An
1291 invertebrate Warburg effect: A shrimp virus achieves successful replication by altering
1292 the host metabolome via the PI3K-Akt-mTOR pathway. PLOS Pathog., 10(6), e1004196.

1293 Surazynski, A., Donald, S.P., Cooper, S.K., Whiteside, M.A., Salnikow, K., Liu, Y., et al.,
1294 2008. Extracellular matrix and HIF-1 signaling: The role of prolidase. Int. J. Cancer,
1295 122(6), 1435–1440.

1296 Surjana, D., Halliday, G.M., Damian, D.L., 2010. Role of nicotinamide in DNA damage,
1297 mutagenesis, and DNA repair. J. Nucleic Acids, Article ID 157591, DOI:
1298 10.4061/2010/157591

1299 Tallam, A., Perumal, T.M., Antony, P.M., Jäger, C., Fritz, J.V., Vallar, L., et al., 2016. Gene
1300 Regulatory Network Inference of Immunoresponsive Gene 1 (IRG1) Identifies Interferon
1301 Regulatory Factor 1 (IRF1) as Its Transcriptional Regulator in Mammalian
1302 Macrophages. PLOS ONE, 11(2), e0149050.

1303 Tamayo, D, Corporeau, C, Petton, B, Quéré, C, Pernet, F., 2014. Physiological changes in
1304 Pacific oyster *Crassostrea gigas* exposed to the herpesvirus OsHV-1 µvar. Aquaculture,
1305 432, 304–310.

1306 Tannahill, G.M., Curtis, A.M., Adamik, J., Palsson-McDermott, E.M., McGettrick, A.F.,
1307 Goel, G., et al., 2013. Succinate is an inflammatory signal that induces IL-1 [bgr]
1308 through HIF-1 [agr]. Nature, 496(7444), 238–242.

1309 Thai, M., Graham, N.A., Braas, D., Nehil, M., Komisopoulou, E., Kurdistani, S.K., et al.,
1310 2014. Adenovirus E4ORF1-induced MYC activation promotes host cell anabolic glucose
1311 metabolism and virus replication. Cell Metab., 19(4), 694–701.

1312 Thai, M., Thaker, S.K., Feng, J., Du, Y., Hu, H., Wu, T.T., et al., 2015. MYC-induced
1313 reprogramming of glutamine catabolism supports optimal virus replication. Nat.
1314 Commun., 6, Article number 8873, DOI: 10.1038/ncomms9873

1315 Thompson, C.B., 2014. Wnt meets Warburg: Another piece in the puzzle? EMBO J., 33(13),
1316 1420–1422.

1317 Tilford, C.A., Siemers, N.O., 2009. Gene set enrichment analysis, in: Nikolsky Y., Bryant J.
1318 (Eds.), Protein Networks and Pathway Analysis. Humana Press, Springer, New York,
1319 USA, pp. 99–121.

1320 Torres, M.A., Jones, J.D., Dangl, J.L., 2006. Reactive oxygen species signaling in response to
1321 pathogens. Plant Physiol., 141(2), 373–378.

1322 Touw, W.G., Bayjanov, J.R., Overmars, L., Backus, L., Boekhorst, J., Wels, M., et al., 2012.
1323 Data mining in the life sciences with Random Forest: A walk in the park or lost in the
1324 jungle? Brief. Bioinform., 14 (3),315-326.

1325 Tretter, L., Patocs, A., Chinopoulos, C., 2016. Succinate, an intermediate in metabolism,
1326 signal transduction, ROS, hypoxia, and tumorigenesis. BBA-Bioenergetics, 1857(8),
1327 1086–1101.

1328 Vander, Heiden, M.G., Cantley, L.C., Thompson, C.B., 2009. Understanding the Warburg
1329 effect: The metabolic requirements of cell proliferation. Science, 324(5930), 1029–1033.

1330 Vijayakumar, S.N., Sethuraman, S., Krishnan, U.M., 2015. Metabolic pathways in cancers:
1331 Key targets and implications in cancer therapy. RSC Adv., 5(52), 41751–41762.

1332 Vuoristo, K.S., Mars, A.E., van Loon, S., Orsi, E., Eggink, G., Sanders, J.P., et al., 2015.
1333 Heterologous expression of *Mus musculus* immunoresponsive gene 1 (irg1) in
1334 *Escherichia coli* results in itaconate production. Front. Microbiol., 6, 849, DOI:
1335 10.3389/fmicb.2015.00849

1336 Vyas, S., Chesarone-Cataldo, M., Todorova, T., Huang, Y.H., Chang, P., 2013. A systematic
1337 analysis of the PARP protein family identifies new functions critical for cell physiology.
1338 Nat. Commun., 4 Article number 2240, DOI: 10.1038/ncomms3240

1339 Wang, T.J., Ngo, D., Psychogios, N., Dejam, A., Larson, M.G., Vasan, R.S., et al., 2013. 2-
1340 Aminoadipic acid is a biomarker for diabetes risk. J. Clin. Invest., 123(10), 4309–4317.

1341 Weljie, A.M., Jirik, F.R., 2011. Hypoxia-induced metabolic shifts in cancer cells: Moving
1342 beyond the Warburg effect. Int. J. Biochem. Cell Biol., 43(7), 981–989.

1343 Whittington, R., Hick, P., Evans, O., Rubio, A., Dhand, N., Paul-Pont, I., 2016. Pacific oyster
1344 mortality syndrome: A marine herpesvirus active in Australia. Microbiol. Aust., 37(3),
1345 126–128.

1346 Winter, G., Krömer, J.O., 2013. Fluxomics–connecting 'omics analysis and phenotypes.
1347 Environ. Microbiol., 15(7), 1901–1916.

1348 Wishart, D.S., 2016. Emerging applications of metabolomics in drug discovery and precision
1349 medicine. Nat. Rev. Drug Discov., 15, 473–484.

1350 Wu, H., Ji, C., Wei, L., Zhao, J., Lu, H., 2013. Proteomic and metabolomic responses in
1351 hepatopancreas of *Mytilus galloprovincialis* challenged by *Micrococcus luteus* and
1352 *Vibrio anguillarum*. J. Proteomics, 94, 54–67.

1353 Xia, J., Wishart, D.S., 2010. MetPA: A web-based metabolomics tool for pathway analysis
1354 and visualization. Bioinformatics, 26(18), 2342–2344.

1355 Xia, J., Wishart, D.S., 2011. Web-based inference of biological patterns, functions and
1356 pathways from metabolomic data using MetaboAnalyst. Nat. Protoc., 6, 743–760.

1357 Xia, J., Bai, C., Wang, C., Song, X., Huang, J., 2015a. Complete genome sequence of Ostreid
1358 herpesvirus-1 associated with mortalities of *Scapharca broughtonii* broodstocks. Virol.
1359 J., 12(1), 110–119.

1360 Xia, J., Sinelnikov, I.V., Han, B., Wishart, D.S., 2015b. MetaboAnalyst 3.0—making
1361 metabolomics more meaningful. Nucleic Acid Res., 43(W1), W251–W257.

1362 Xiong, X., Sheng, X., Liu, D., Zeng, T., Peng, Y., Wang, Y., 2015. A GC/MS-based
1363 metabolomic approach for reliable diagnosis of phenylketonuria. Anal. Bioanal. Chem.,
1364 407(29), 8825–8833.

1365 Yamamoto, K., Nagata, K., Ohara, H., Aso, Y., 2015. Challenges in the production of
1366 itaconic acid by metabolically engineered *Escherichia coli*. Bioengineered, 6(5), 303–
1367 306.

1368 Ye, Y., Xia, M., Mu, C., Li, R., Wang, C., 2016. Acute metabolic response of *Portunus*
1369 *trituberculatus* to *Vibrio alginolyticus* infection. Aquaculture, 463, 201–208.

1370 Yoshino, T.P., Bickham, U., Bayne, C.J., 2013. Molluscan cells in culture: Primary cell
1371 cultures and cell lines 1. Can. J. Zool., 91(6), 391–404.

1372 Young, T., Alfaro, A.C., Villas-Boas, S.G., 2015. Identification of candidate biomarkers for
1373 quality assessment of hatchery-reared mussel larvae via GC/MS-based metabolomics. N.
1374 Z. J. Mar. Freshwater Res., 49(1), 87–95.

1375 Young, T., Alfaro, A.C., 2016. Metabolomic strategies for aquaculture research: A primer.
1376 Rev. Aquacult., DOI: 10.1111/raq.12146

1377 Young, T., Alfaro, A.C., Villas-Boas, S.G., 2016. Metabolic profiling of mussel larvae:
1378 Effect of handling and culture conditions. Aquacult. Int., 24(3), pp. 843–856.

1379 Yuan, W., Zhang, J., Li, S., Edwards, J.L., 2011. Amine metabolomics of hyperglycemic
1380 endothelial cells using capillary LC–MS with isobaric tagging. J. Proteome Res., 10(11),
1381 5242–5250.

1382 Yuasa, H.J., Ball, H.J., 2015. Efficient tryptophan-catabolizing activity is consistently
1383 conserved through evolution of TDO enzymes, but not IDO enzymes. J. Exp. Zool. B
1384 Mol. Dev. Evol., 324(2), 128–140.

1385 Yuasa, H.J., Mizuno, K., Ball, H.J., 2015. Low efficiency IDO2 enzymes are conserved in
1386 lower vertebrates, whereas higher efficiency IDO1 enzymes are dispensable. FEBS J.,
1387 282(14), 2735–2745.

1388 Zaidi, N., Lupien, L., Kuemmerle, N.B., Kinlaw, W.B., Swinnen, J.V., Smans, K., 2013.
1389 Lipogenesis and lipolysis: The pathways exploited by the cancer cells to acquire fatty
1390 acids. Prog. Lipid Res., 52(4), 585–589.

1391 Zeitoun-Ghandour, S., Leszczyszyn, O.I., Blindauer, C.A., Geier, F.M., Bundy, J.G.,
1392 Stürzenbaum, S.R., 2011. *C. elegans* metallothioneins: Response to and defence against
1393 ROS toxicity. Mol. Biosyst., 7(8), 2397–2406.

1394 Zhang, J., Nuebel, E., Daley, G.Q., Koehler, C.M., Teitell, M.A., 2012. Metabolic regulation
1395 in pluripotent stem cells during reprogramming and self-renewal. Cell Stem Cell, 11(5),
1396 589–595.

1397 Zhao, X.L., Han, Y., Ren, S.T., Ma, Y.M., Li, H., Peng, X.X., 2015. L-proline increases
1398 survival of tilapias infected by *Streptococcus agalactiae* in higher water temperature.
1399 Fish Shellfish Immunol., 44(1), 33–42.

Figure 1. Metabolites detected as being significantly different ($p < 0.05$) between control and OsHV-1 µVar-infected larvae. (A) Significant Analysis of Metabolites (SAM) plot. (B) Empirical Bayes Analysis of Metabolites (EBAM) plot. (C) Summary of statistically different metabolite levels between treatment groups with their respective Log_2 fold change values (virus-infected [red circles] / control [green circles] larvae).

Figure 2. Unsupervised multivariate cluster analyses of metabolite profiles from larvae infected with OsHV-1 µVar vs control larvae. (A) Hierarchical Cluster Analysis (Euclidian distance; Ward's method). (B) Table of results from *k*-Means cluster analysis where k clusters = 2 (C*n* = control sample *n*; V*n* = virus-infected sample *n*). (C) Principal Component Analysis (PCA) score plot. (D) PCA scree plot showing variation explained by *n* PC (blue line), and the cumulative variance explained in *n* PC's (green line).

Figure 3. Supervised multivariate classification analyses of metabolite profiles from larvae infected with OsHV-1 µVar vs control larvae. (A) Projection to Latent Structure Discriminant Analysis (PLS-DA) score plot with accuracy of 100%, multiple correlation coefficient (R^2) of 96.9%, and cross-validated R^2 (Q^2) of 79.6%. (B) Variable Importance in Projection (VIP) scores for the PLS-DA model.

Figure 4. Multivariate machine learning and predictive modelling of larval sample classes via Random Forest (RF) analysis with Monte-Carlo Cross Validation (MCCV). (A) Predictive accuracies of RF models with different *n* features. (B) Area Under Curve (AUC) generated from Receiver Operating Characteristic (ROC) curve analysis of RF models with 5, 10, 15, 25, 50 and 100 features. (C) AUC of the 5-feature RF model. (D) Predicted class probabilities (average of the MCCV) for each sample using the best classifiers (based on AUC) of the 5-feature RF model. (E) The average importance of metabolites in the 5-feature RF model based on ROC curve analysis, with the most discriminating feature in descending order of importance. (F) The selected frequencies of metabolites in the 5-feature RF model based on ROC curve analysis.

Figure 5. Secondary bioinformatics of annotated metabolites. (A) Topology-based pathway analysis showing metabolic networks in oyster larvae potentially affected by OsHV-1 µVar. The most impacted metabolic pathways are specified by the volume and the colour of the spheres (yellow = least relevant; red = most relevant) according to their statistical relevance and pathway impact (PI) values resulting from Quantitative Enrichment Analysis (QTA) and Network Topology Analysis (NTA), respectively. (B–E) Examples of four pathways containing relatively high metabolite coverages: (B) Tricarboxylic acid cycle ($p < 0.001$, FDR < 0.000, PI = 0.26); (C) Alanine, aspartate and glutamate metabolism ($p < 0.001$, FDR = 0.002, PI = 0.72); (D) Glutathione metabolism ($p = 0.057$, FDR = 0.107, PI = 0.48); (E) Cysteine and methionine metabolism ($p = 0.033$, FDR = 0.076, PI = 0.60). Boxes which vary from yellow to red represent metabolites (KEGG ID codes) that were detected and annotated with our methods. Their colour indicates the level of significance (light yellow: $p > 0.05$, light orange to red: $p < 0.05$) from unpaired *t*-tests (control vs treatment). Light blue boxes/compounds in the pathways were not detected, but were used as background information for QEA to calculate the proportion of identified compounds within each pathway, and in NTA to determine the position (relative-betweeness centrality) and importance of each metabolite.

Figure 6. Metabolite–metabolite Pearson correlation heatmaps of healthy control larvae (A) vs. unhealthy virus-exposed larvae (B). The order of metabolites are the same for each of the heatmaps so direct comparisons can be made for particular regions.

Figure 7. Correlation Network Analysis of control (A) vs. virus exposed larvae (B). Metabolite–metabolite Pearson correlations > 0.9 are represented by grey solid lines, whereas those that are < -0.9 are represented by dashed grey lines.

Supplementary Table 1. List of identified metabolites showing the effect of OsHV-1 infection on oyster larvae. Up and down arrows represent metabolite levels which were identified as being significantly higher or lower in the virus infected group compared to control animals (via t-test, SAM and/or EBAM), or with high (> 1.0) Variable of Importance (VIP) scores in the PLS-DA model.

Supplementary Table 2. List of unannotated metabolites showing the effect of OsHV-1 infection on oyster larvae. Up and down arrows represent metabolite levels which were identified as being significantly higher or lower in the virus infected group compared to control animals (via t-test, SAM and/or EBAM), or with high (> 1.0) Variable of Importance (VIP) scores in the PLS-DA model.

Supplementary Table 3. List of altered metabolic pathways in larval hosts during viral (OsHV-1 µVar) infection.

Figure 1.

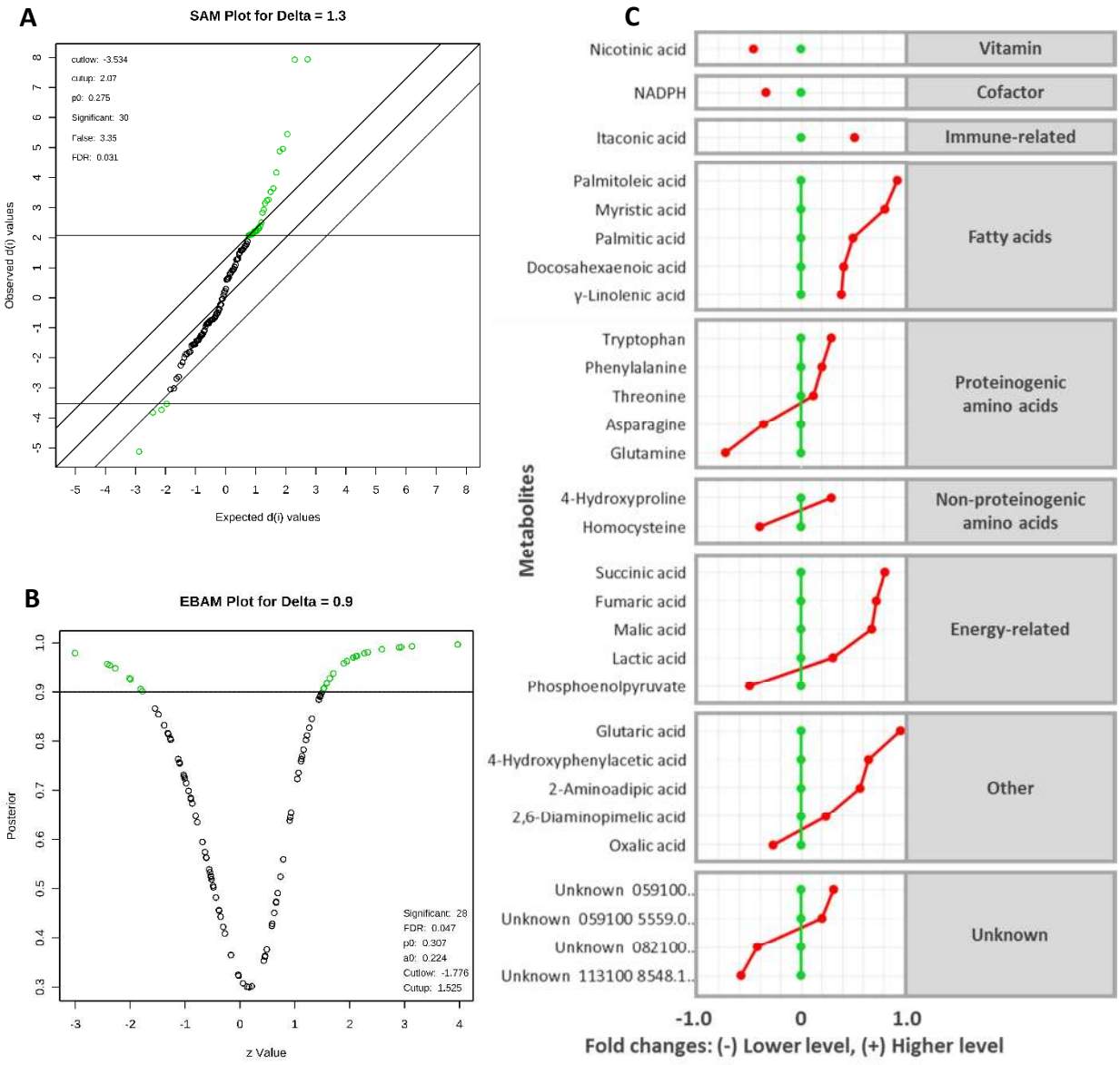
A
SAM Plot for Delta = 1.3
cutlow: -3.534
cutup: 2.07
p0: 0.275
Significant: 30
False: 3.35
FDR: 0.031
Observed d(i) values
Expected d(i) values
B
EBAM Plot for Delta = 0.9
Significant: 28
FDR: 0.047
p0: 0.307
a0: 0.224
Cutlow: -1.776
Cutup: 1.525
Posterior
z Value
C
Nicotinic acid
NADPH
Itaconic acid
Palmitoleic acid
Myristic acid
Palmitic acid
Docosahexaenoic acid
γ-Linolenic acid
Tryptophan
Phenylalanine
Threonine
Asparagine
Glutamine
4-Hydroxyproline
Homocysteine
Succinic acid
Fumaric acid
Malic acid
Lactic acid
Phosphoenolpyruvate
Glutaric acid
4-Hydroxyphenylacetic acid
2-Aminoadipic acid
2,6-Diaminopimelic acid
Oxalic acid
Unknown 059100..
Unknown 059100 5559.0..
Unknown 082100..
Unknown 113100 8548.1..
Metabolites
Vitamin
Cofactor
Immune-related
Fatty acids
Proteinogenic amino acids
Non-proteinogenic amino acids
Energy-related
Other
Unknown
-1.0
0
1.0
Fold changes: (-) Lower level, (+) Higher level

Figure 2.

A

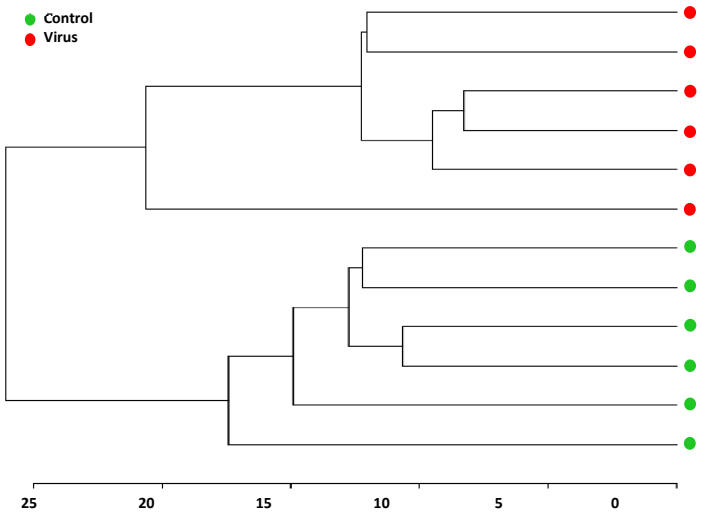

B

Sample partitioning	
Group 1:	C1, C2, C3, C4, C5, C6
Group 2:	V1, V2, V3, V4, V5, V6
Accuracy:	100 %

C

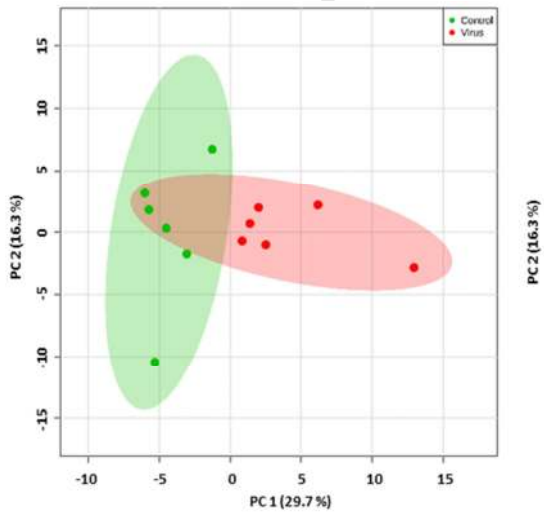

D

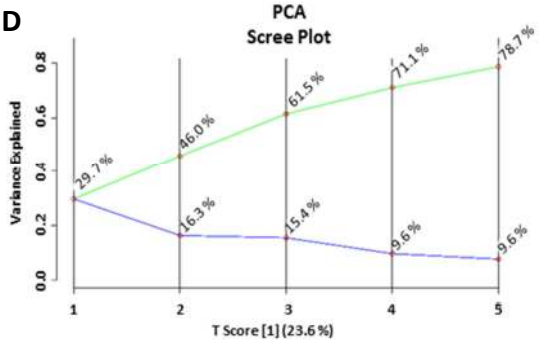

Figure 3.

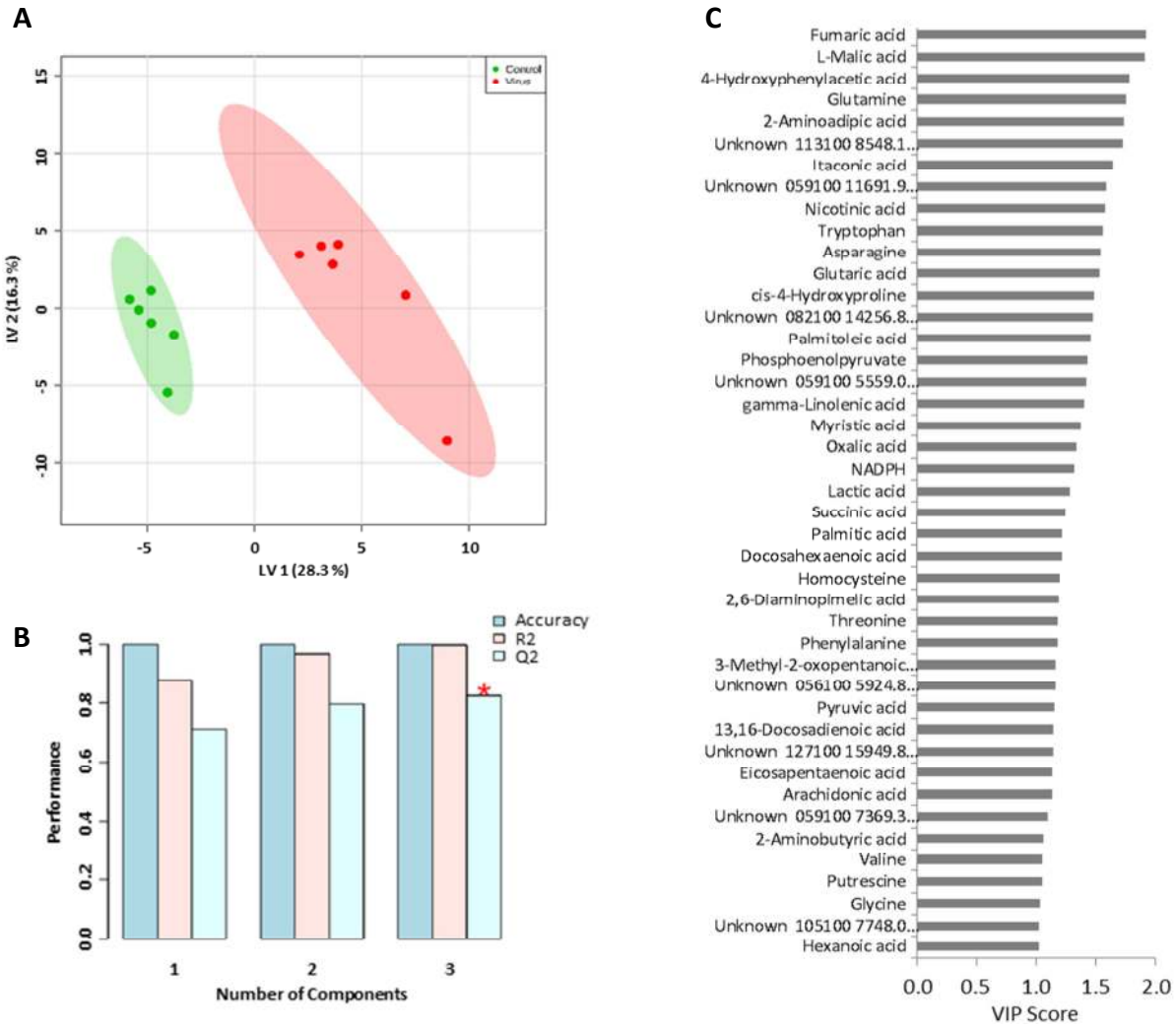
A
Control
Virus
LV 2 (16.3 %)
LV 1 (28.3 %)
B
Accuracy
R2
Q2
Performance
Number of Components
C
Fumaric acid
L-Malic acid
4-Hydroxyphenylacetic acid
Glutamine
2-Aminoadipic acid
Unknown 113100 8548.1...
Itaconic acid
Unknown 059100 11691.9...
Nicotinic acid
Tryptophan
Asparagine
Glutaric acid
cis-4-Hydroxyproline
Unknown 082100 14256.8...
Palmitoleic acid
Phosphoenolpyruvate
Unknown 059100 5559.0...
gamma-Linolenic acid
Myristic acid
Oxalic acid
NADPH
Lactic acid
Succinic acid
Palmitic acid
Docosahexaenoic acid
Homocysteine
2,6-Diaminopimelic acid
Threonine
Phenylalanine
3-Methyl-2-oxopentanoic...
Unknown 056100 5924.8...
Pyruvic acid
13,16-Docosadienoic acid
Unknown 127100 15949.8...
Eicosapentaenoic acid
Arachidonic acid
Unknown 059100 7369.3...
2-Aminobutyric acid
Valine
Putrescine
Glycine
Unknown 105100 7748.0...
Hexanoic acid
VIP Score

Figure 4.

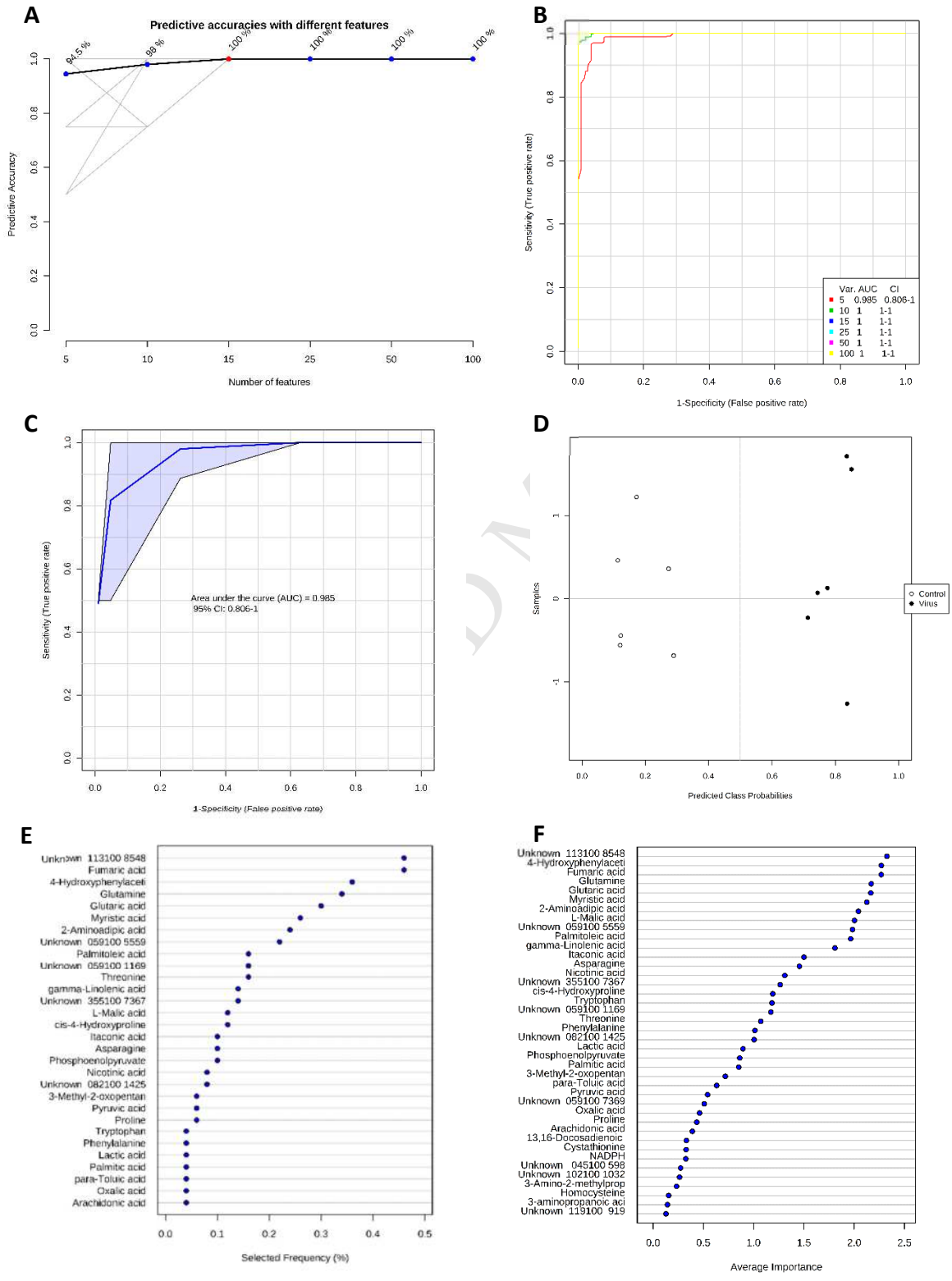
A
Predictive accuracies with different features
84.5 %
98 %
100 %
100 %
100 %
100 %
Predictive Accuracy
Number of features
B
Sensitivity (True positive rate)
1-Specificity (False positive rate)
Var. AUC CI
5 0.985 0.806-1
10 1 1-1
15 1 1-1
25 1 1-1
50 1 1-1
100 1 1-1
C
Sensitivity (True positive rate)
1-Specificity (False positive rate)
Area under the curve (AUC) = 0.985
95% CI: 0.806-1
D
Samples
Predicted Class Probabilities
Control
Virus
E
Unknown 113100 8548
Fumaric acid
4-Hydroxyphenylaceti
Glutamine
Glutaric acid
Myristic acid
2-Aminoadipic acid
Unknown 059100 5559
Palmitoleic acid
Unknown 059100 1169
Threonine
gamma-Linolenic acid
Unknown 355100 7367
L-Malic acid
cis-4-Hydroxyproline
Itaconic acid
Asparagine
Phosphoenolpyruvate
Nicotinic acid
Unknown 082100 1425
3-Methyl-2-oxopentan
Pyruvic acid
Proline
Tryptophan
Phenylalanine
Lactic acid
Palmitic acid
para-Toluic acid
Oxalic acid
Arachidonic acid
Selected Frequency (%)
F
Unknown 113100 8548
4-Hydroxyphenylaceti
Fumaric acid
Glutamine
Glutaric acid
Myristic acid
2-Aminoadipic acid
L-Malic acid
Unknown 059100 5559
Palmitoleic acid
gamma-Linolenic acid
Itaconic acid
Asparagine
Nicotinic acid
Unknown 355100 7367
cis-4-Hydroxyproline
Tryptophan
Unknown 059100 1169
Threonine
Phenylalanine
Unknown 082100 1425
Lactic acid
Phosphoenolpyruvate
Palmitic acid
3-Methyl-2-oxopentan
para-Toluic acid
Pyruvic acid
Unknown 059100 7369
Oxalic acid
Proline
Arachidonic acid
13,16-Docosadienoic
Cystathionine
NADPH
Unknown 045100 598
Unknown 102100 1032
3-Amino-2-methylprop
Homocysteine
3-aminopropanoic aci
Unknown 119100 919
Average Importance

Figure 5.

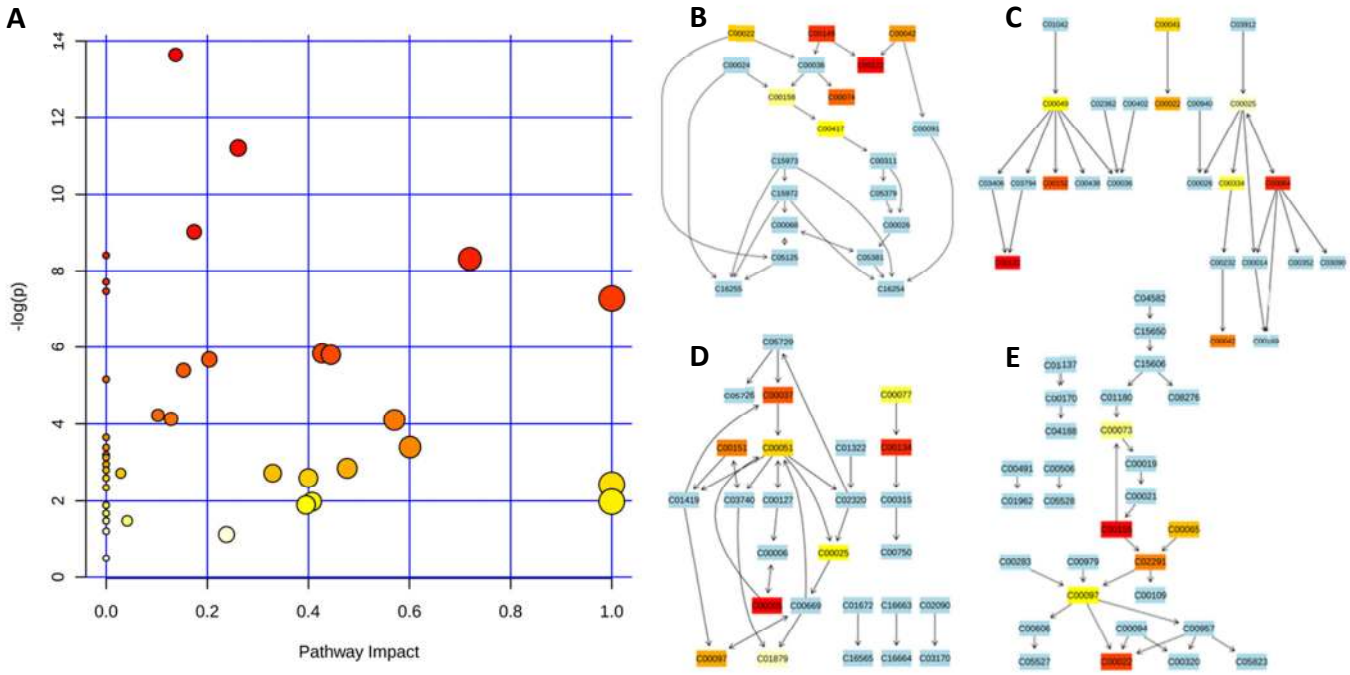

Figure 6.

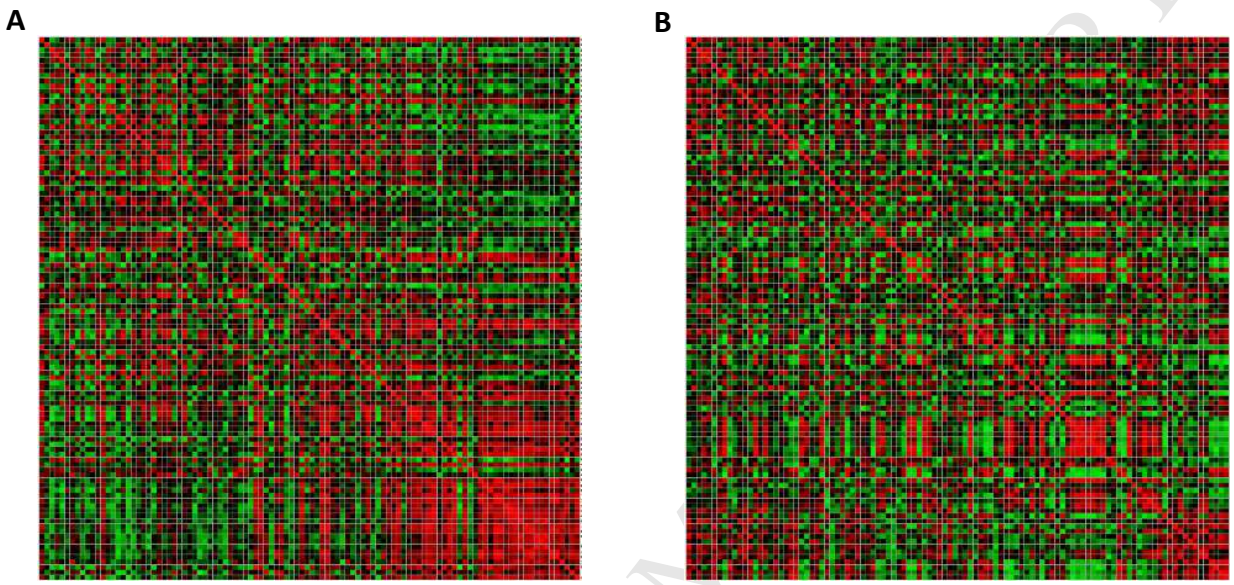

Figure 7.

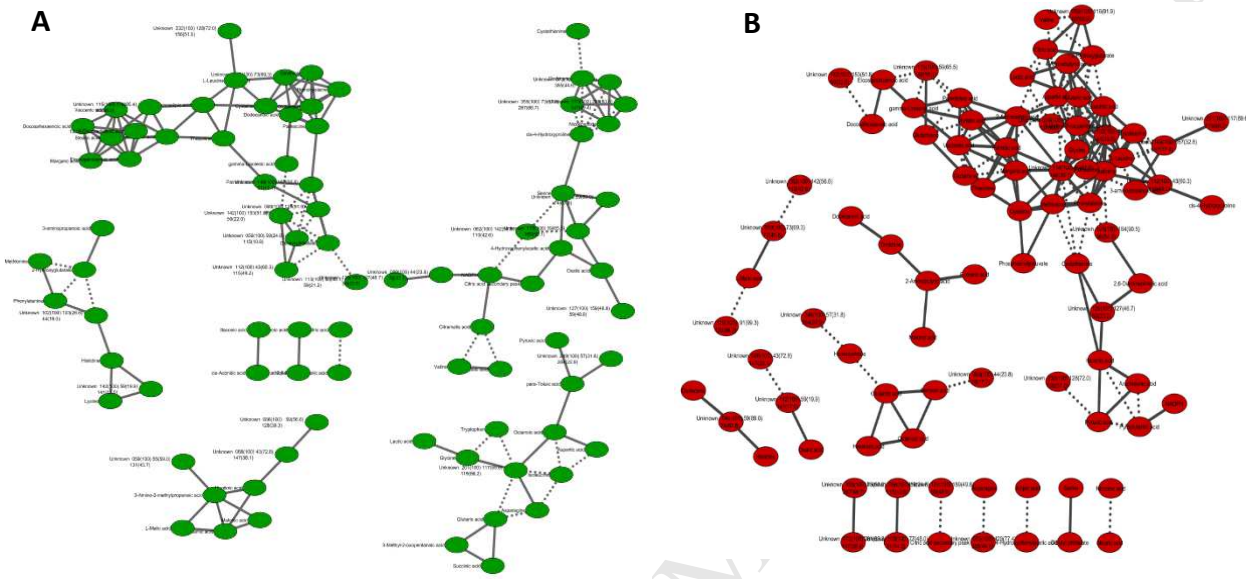

HIGHLIGHTS

- Herpesvirus-induced metabolic responses were investigated in oyster larvae by GC-MS
- Host metabolism changes are suggestive of Irg-1-like activation
- Energy and lipid metabolism was substantially disturbed during infection
- Activation of immunoresponsive gene 1 and the Warburg effect is hypothesised
- Metabolomics is a powerful approach to study disease in early oyster life stage